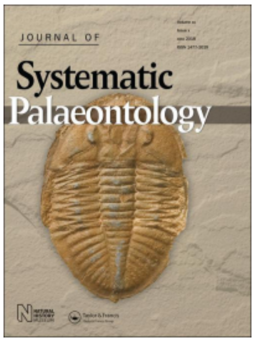

Journal of Systematic Palaeontology

ISSN: (Print) (Online) Journal homepage: www.tandfonline.com/journals/tjsp20

Evidence of large-sized ankylopollexian dinosaurs (Ornithischia: Iguanodontia) in the Upper Jurassic of Portugal

Filippo Maria Rotatori, Fernando Escaso, Bruno Camilo, Filippo Bertozzo, Elisabete Malafaia, Octávio Mateus, Pedro Mocho, Francisco Ortega & Miguel Moreno-Azanza

To cite this article: Filippo Maria Rotatori, Fernando Escaso, Bruno Camilo, Filippo Bertozzo, Elisabete Malafaia, Octávio Mateus, Pedro Mocho, Francisco Ortega & Miguel Moreno-Azanza (2025) Evidence of large-sized ankylopollexian dinosaurs (Ornithischia: Iguanodontia) in the Upper Jurassic of Portugal, Journal of Systematic Palaeontology, 23:1, 2470789, DOI: 10.1080/14772019.2025.2470789

To link to this article: https://doi.org/10.1080/14772019.2025.2470789

Journal of Systematic Palaeontology, 2025
Vol. 23, No. 1, 2470789
http://dx.doi.org/10.1080/14772019.2025.2470789

Evidence of large-sized ankylopollexian dinosaurs (Ornithischia: Iguanodontia) in the Upper Jurassic of Portugal

Filippo Maria Rotatori[a,b†]*, Fernando Escaso[c,d†], Bruno Camilo[a,d,e‡], Filippo Bertozzo[f,d], Elisabete Malafaia[g,c,d], Octávio Mateus[a,b], Pedro Mocho[g,c,d], Francisco Ortega[c,d] and Miguel Moreno-Azanza[a,b,h]

[a]GEOBIOTEC, Department of Earth Sciences, NOVA School of Science and Technology, Universidade NOVA de Lisboa, P-2829 516 Campus de Caparica, Caparica, Portugal; [b]Museu da Lourinhã, Rua João Luis de Moura 95, 2530-158 Lourinhã, Portugal; [c]Grupo de Biología Evolutiva, Universidad Nacional de Educación a Distancia (UNED), Avda.Esparta s/n, 28232 Las Rozas de Madrid, Spain; [d]Laboratório de Paleontologia e Paleoecologia, Sociedade de História Natural, Polígono Industrial do Alto do Ameal, Pav. H02 e H06, 2565-641, Torres Vedras, Portugal, Portugal; [e]European Centre of Paleontology, Institute of Biology, Laboratory of Paleobiology, University of Opole, ul.Oleska 48, 45-052 Opole, Poland; [f]Operational Directorate Earth and History of Life, Royal Belgian Institute of Natural Sciences, Brussels, Belgium; [g]Instituto Dom Luiz, Faculdade de Ciências da Universidade de Lisboa, Campo Grande Edifício C1 Piso 1,1749-016 Lisboa, Portugal; [h]Aragosaurus: Recursos Geológicos y Paleoambientes-IUCA, Facultad de Ciencias, Universidade de Zaragoza, 50009, Zaragoza, Spain

(Received 14 March 2023; accepted 28 January 2025)

The Upper Jurassic beds of the Lusitanian Basin in central Portugal yield diverse dinosaurian fauna, dated to the Kimmeridgian–Tithonian interval. Saurischian dinosaurs are, overall, more abundant than their ornithischian counterparts, in terms of both specimens collected and species recognized. Iguanodontians are so far represented by the styracosternan *Draconyx loureiroi*, the dryosaurid *Eousdryosaurus nanohallucis* and the enigmatic dryomorphan *Hesperonyx martinhotomasorum.* Here we aim to highlight the diversity of this clade in the Late Jurassic of Portugal, presenting evidence for yet another species of ankylopollexian iguanodontian dinosaur, represented by the specimen SHN.JJS.015, which is housed at the Sociedade de História Natural, Torres Vedras. Detailed comparisons rule out attribution to previously known taxa, and phylogenetic analyses that include SHN.JJS.015 indicate early-diverging ankylopollexian affinities for this specimen. As there is no robust diagnosis, we do not erect a new formal species for it at this stage. Nevertheless, this specimen represents a previously unreported taxon that highlights greater diversity than previously estimated among the iguanodontians of the Late Jurassic and highlights the importance of Europe in diversification and dispersal events of this clade. A series of smaller, isolated femora from the same sub-basin as SHN.JJS.015 may represent the same taxon, presenting evidence of thriving communities of ankylopollexians during the Kimmeridgian–Tithonian interval in Portugal.

Keywords: Systematics; palaeobiodiversity; Ornithopoda; Lusitanian Basin; Iberian Peninsula; Late Jurassic

Introduction

The Upper Jurassic beds of the Lusitanian Basin have yielded a diverse fauna of terrestrial vertebrates (Mateus et al., 2017, Ortega, 2009). Despite the lack of consensus on the definition and use of the formal lithostratigraphic units, these beds are considered by several researchers to be Kimmeridgian–Tithonian in age (Fürsich, 1981; Fürsich et al., 2022; Hill, 1988; Manuppella, 1998; Mateus et al., 2017; Mocho, Royo-Torres, Escaso et al., 2017; Taylor et al., 2014). The vertebrate fauna recovered from the Upper Jurassic of the Lusitanian Basin consists of dinosaurs, pterosaurs, crocodyliforms, turtles, amphibians, lepidosaurs, mammaliaforms and fishes (Bertozzo et al., 2021; Guillaume et al., 2020, 2022; López-Rojas et al., 2024; Mateus et al., 2017; Ortega, 2009). Among the dinosaurs, theropod and sauropod taxa have been shown to be highly diverse (Antunes & Mateus, 2003; Malafaia et al., 2020; Mateus, 1998; Mateus et al., 2014; Mocho et al., 2014, 2016, 2019; Mocho, Royo-Torres, Escaso et al., 2017; Mocho, Royo-Torres, Malafaia, et al., 2017), whereas ornithischians have traditionally been considered less diverse (Costa & Mateus, 2019; Escaso et al., 2007, 2014; Mateus & Antunes, 2001; Mateus et al., 2009; Thulborn, 1973), with only six species formally named: three ornithopods and three thyreophorans.

---

*Corresponding author. Email: filippo.rotatori.93@gmail.com
†These authors contributed equally to this work.
‡Additional affiliation: Departamento de Engenharia de Recursos Minerais e Energéticos, Instituto Superior Técnico, Universidade de Lisboa. Av. Rovisco Pais, 1 1049-001 Lisboa, Portugal.

Iguanodontian ornithopods are represented so far by the dryosaurid *Eousdryosaurus nanohallucis*, the ankylopollexian *Draconyx loureiroi* and the enigmatic *Hesperonyx martinhotomasorum* (Escaso et al., 2014; Mateus & Antunes, 2001; Rotatori et al., 2022, 2023), although reconsideration of several lines of evidence indicates that the diversity of this group has been largely underestimated (Castanera et al., 2020; Rotatori et al., 2020). Various other isolated remains can be ascribed to indeterminate ankylopollexians or dryosaurids (Rotatori et al., 2020, 2024). In other parts of the Iberian Peninsula, more precisely in the municipality of Riodeva (Teruel, Spain), the basal ankylopollexian *Oblitosaurus bunnueli* has recently been described (Sánchez-Fenollosa et al., 2023) from the Villar del Arzobispo Formation (Kimmeridgian–Berriasian).

The fossil record of early-diverging iguanodontians dated to the Jurassic is very poor in Europe, with only *Callovosaurus leedsi* (Ruiz-Omeñaca et al., 2006) and *Cumnoria prestwichii* (Galton & Powell, 1980; Maidment et al., 2022) recognized as species in the United Kingdom. In the United States, the Morrison Formation, despite its high number of specimens, has produced only *Camptosaurus dispar* and *Uteodon aphanoecetes* as ankylopollexian species (Foster, 2020). Given the wide chronostratigraphic range of the Morrison Formation (Foster, 2020), it is likely that the diversity of iguanodontians has been underestimated. *Camptosaurus*, as considered by Carpenter and Wilson (2008) to include the species '*Camptosaurus aphanoecetes*', ranges from Oxfordian to mid-Tithonian, whereas *Uteodon* is limited to the Tithonian stage. Dryosaurids in the Morrison Formation are represented only by *Dryosaurus*, which includes the species *D. altus* and *D. elderae* (Carpenter & Galton, 2018). *Dryosaurus* spp. also displays an extensive stratigraphic distribution, ranging from the Kimmeridgian to the Tithonian (Carpenter & Galton, 2018).

Here we contribute to unveiling the diversity of iguanodontian dinosaurs in the Late Jurassic of Portugal, recognizing a previously unrecognized early-diverging ankylopollexian taxon based on previously described materials (Escaso, 2014; Mateus & Antunes, 2001; Rotatori et al., 2020, 2022).

Geological context

The sedimentary sequence of the Lusitanian Basin, located in the western region of the Iberian Peninsula, was deposited from the Middle Triassic (?Ladinian–Carnian) (Rocha et al., 1996) to the Late Cretaceous (Turonian) (Rey, 1999) (see Fig. 1). The Upper Jurassic sedimentary sequence represents a third rifting episode (Kullberg et al., 2013; Rasmussen et al., 1998), marked by intense subsidence and an internal differentiation into three main sectors (Rocha & Soares, 1984): (i) the northern sector extends from Coimbra to the Nazaré Fault and is characterized by lower subsidence than the central sector; (ii) the central sector extends from this main tectonic line to the Lisbon area and presents the maximum subsidence; and (iii) the southern sector extends from Lisbon to the alpine Arrábida Chain and shows the lowest subsidence. This episode of rifting was marked by a major sedimentary input into the whole basin, which progressively filled the basin (e.g. Kullberg et al., 2013; Pena dos Reis et al., 2000). The central sector of the Lusitanian Basin has recently been divided into distinct sub-basins (e.g. Fürsich et al., 2022; Kulberg et al., 2013; Taylor et al., 2014). From the lower Kimmeridgian to the top of the Upper Jurassic, the sedimentary sequence was dominated by abundant siliciclastic inputs, with a primarily continental and transitional signature (e.g. Hill, 1988; Manuppella et al., 1999), and was mainly deposited in distal fluvio-deltaic to coastal environments, producing the richest fossil record of terrestrial vertebrates in the Lusitanian Basin (e.g. Lapparent & Zbyszewski, 1957; Mateus et al., 2017; Ortega et al., 2009). The stratigraphy of the Upper Jurassic sequence of the Lusitanian Basin is complex owing to the profuse lateral heterogeneity and the variety of stratigraphic approaches that have been proposed (e.g. Fürsich et al., 2022; Hill, 1988; Leinfelder, 1986; Manuppella et al., 1999; Mateus et al., 2017; Mocho, Royo-Torres, Escaso et al., 2017; Taylor et al., 2014).

All the specimens presented here were collected in the Upper Jurassic deposits cropping out in the coastal region of Torres Vedras-Lourinhã-Peniche, which is located in the Consolação sub-basin (Taylor et al., 2014). Historically, there is no consensus on the names of the lithostratigraphic units used to refer to the Upper Jurassic outcrops in this area, especially in the southernmost deposits around the municipality of Torres Vedras. Throughout this manuscript, therefore, we will use the two most commonly adopted proposals (Hill, 1988; Manuppella et al., 1999). Specimen SHN.JJS.015 was found in the cliffs of Praia da Corva (municipality of Torres Vedras), belonging to the Praia da Amoreira-Porto Novo Formation (*sensu* Manuppella et al., 1999), or the Porto Novo Member of the Lourinhã Formation (*sensu* Hill, 1988), late Kimmeridgian–earliest Tithonian in age (Manuppella et al., 1999). All the elements referred to this specimen were found in association in the same micaceous coarse-grained grey sandstone level associated with small and carbonized plant debris. Specimen SHN.JJS.073 was collected at Peralta (municipality of Lourinhã) and comes from the sedimentary deposits of the Sobral Formation (*sensu* Manuppella et al., 1999), equivalent to the Praia Azul Member of the Lourinhã Formation

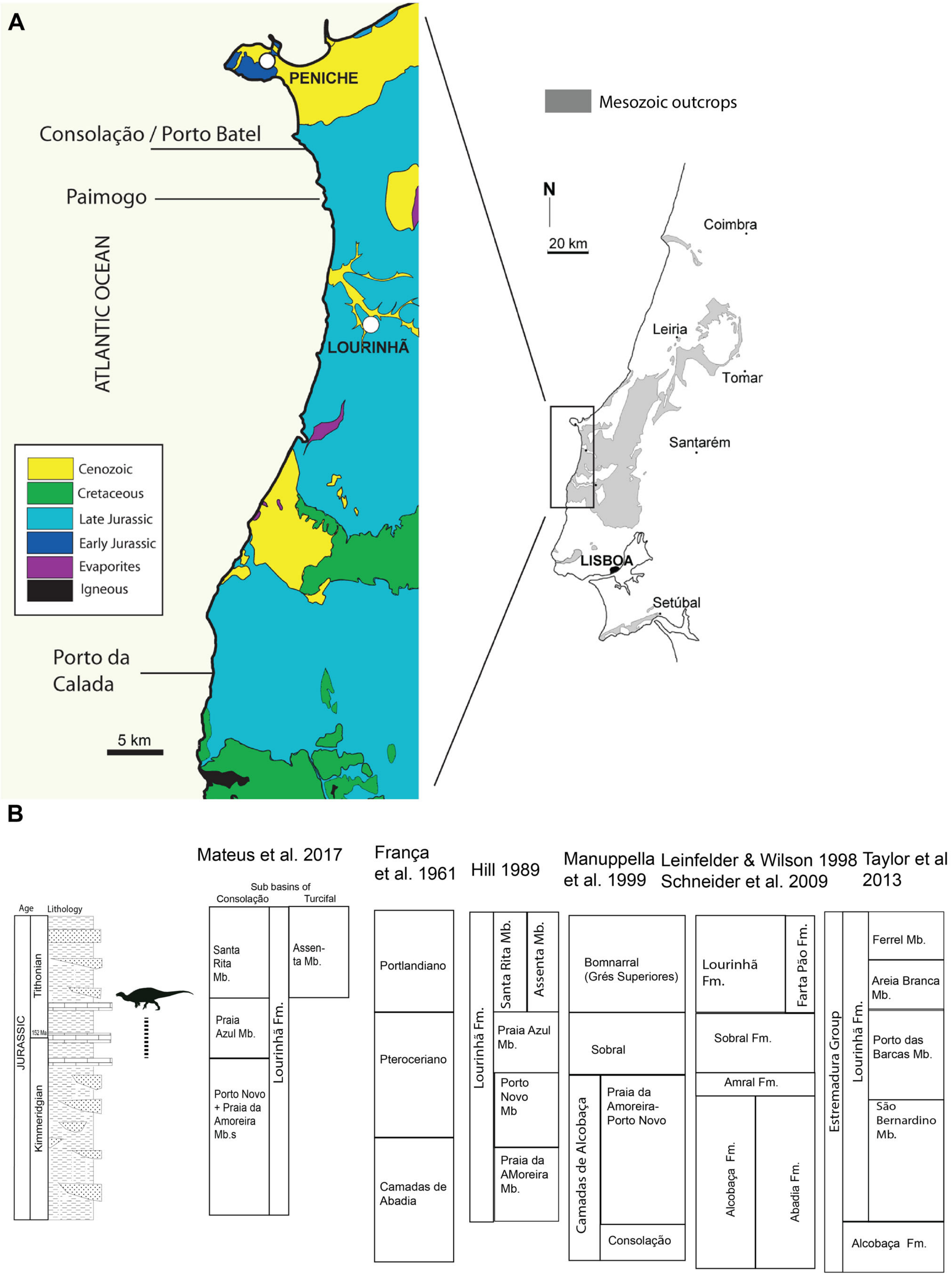
A
PENICHE
Consolação / Porto Batel
Paimogo
ATLANTIC OCEAN
LOURINHÃ
Cenozoic
Cretaceous
Late Jurassic
Early Jurassic
Evaporites
Igneous
Porto da Calada
5 km
Mesozoic outcrops
N
20 km
Coimbra
Leiria
Tomar
Santarém
LISBOA
Setúbal
B
Age
Lithology
JURASSIC
Tithonian
152 Ma
Kimmeridgian
Mateus et al. 2017
Sub basins of
Consolação
Turcifal
Santa Rita Mb.
Praia Azul Mb.
Porto Novo + Praia da Amoreira Mb.s
Lourinhã Fm.
Assen-ta Mb.
França et al. 1961
Portlandiano
Pteroceriano
Camadas de Abadia
Hill 1989
Lourinhã Fm.
Santa Rita Mb.
Assenta Mb.
Praia Azul Mb.
Porto Novo Mb
Praia da AMoreira Mb.
Manuppella et al. 1999
Bomnarral (Grés Superiores)
Sobral
Camadas de Alcobaça
Praia da Amoreira-Porto Novo
Consolação
Leinfelder & Wilson 1998 Schneider et al. 2009
Lourinhã Fm.
Farta Pão Fm.
Sobral Fm.
Amral Fm.
Alcobaça Fm.
Abadia Fm.
Taylor et al 2013
Estremadura Group
Lourinhã Fm.
Ferrel Mb.
Areia Branca Mb.
Porto das Barcas Mb.
São Bernardino Mb.
Alcobaça Fm.

(*sensu* Hill, 1988), which is late Kimmeridgian–early Tithonian in age (Fürsich, 1981). Specimens ML 434 from Praia do Caniçal and ML 2055 from Praia do Zimbral (both in the municipality of Lourinhã) were collected in sediments of the Sobral Formation (*sensu* Manuppella et al., 1999; the Praia Azul Member of the Lourinhã Formation *sensu* Hill, 1988), late Kimmeridgian–early Tithonian in age (Hill, 1988).

Material and methods

The materials presented here were recovered from various localities in western Portugal, in the municipalities of Lourinhã and Torres Vedras. The specimens are held in the Museu da Lourinhã (ML) and the Sociedade de História Natural de Torres Vedras (SHN). To test the affinities of the described specimens, we modified the data set of Xu et al. (2018), adding postcranial characters from Dieudonné et al. (2020), Prieto-Marquez et al. (2019) and Takasaki et al. (2020) resulting in a matrix that includes a total of 171 characters for 43 taxa. The character list and the TNT file are provided in the Supplemental material. The data set was analysed with the software TNT v. 1.5 (Goloboff & Catalano, 2016). A heuristic search with 1000 replicates was performed, keeping 10 trees per replicate. To explore the tree space better, the trees found with the initial search were subjected to another round of tree bisection and reconnection (TBR). It is important to note that the genus *Camptosaurus* has not always been recovered as monophyletic in previous phylogenetic analyses (McDonald, 2012; Poole, 2022; Rotatori et al., 2022; Verdú et al., 2018). Bearing other taxonomic hypotheses in mind (Carpenter & Lamanna, 2015; Sánchez-Fenollosa et al., 2023), we prefer to refer each species (i.e. *Camptosaurus dispar*, *Cumnoria prestwichii* and *Uteodon aphanoecetes*) to a separate genus, pending future works that achieve a better understanding of the systematic relationships of all the species previously included in *Camptosaurus*.

Selected measurements of the specimens described here are provided in Table 1. We estimated the mass of SHN.JJS.015, applying isometric scaling as in supplement S.3 of the paper by Chiarenza et al. (2021), using as a reference the total length of the femur USNM 5473 referred to *Camptosaurus dispar* and associating it with the mass estimated for the species by Benson et al. (2018). Having estimated the size of individual SHN.JJS.015, we used the same approach to estimate the mass of ML 434, SHN.JJS.073 and ML 2055. The specific formula is the following:

$$ms = \left(\frac{xS}{xs}\right)^3 \times mS \tag{1}$$

where x is the length of the skeletal element in question, S is the species (in this case, individual) with a known body mass, s is the species (in this case, individual) with an unknown body mass, and m is the body mass.

Following Rotatori et al. (2022, 2023), moreover, we employed the regression equation to estimate the body length of the specimens reported here.

We employed the following equation assuming a cursorial mode of locomotion:

$$\mathrm{bl} = 0.17 + 9.02 \times (\mathrm{f}) \tag{2}$$

and the following equation assuming a subcursorial mode of locomotion:

$$\mathrm{bl} = 163.63 + 7.54 \times (\mathrm{f}) \tag{3}$$

where bl is body length and f is the femoral shaft length.

Table 1. Selected measurements in mm of the specimens described here. **Abbreviations: An**, anterior; **d**, distal; **H**, height; **ML**, mediolateral; **NSH**, neural spine height; **p**, proximal; **Po**, posterior; **TL**, total length; **TP**, transverse process; **W**, width.

	TL	PoW	PoH	AnW	AnH	NSH	TP	DW	DH	PW	PH
SHN.015											
Dorsal vertebra	70	75	75	73	74	160	75				
Scapula	430								120	100	180
Humerus	360							75	40	120	45
Femur	600							170	140	110	120
Calcaneum	75								50		
ML 434											
Femur	400										
SHN.073											
Femur	260							60	60	60	30

◄

Figure 1. Geographical and stratigraphic context of the material reported here. (**A**) location of the outcrops dated to the Upper Jurassic of the Lusitanian Basin. (**B**) Stratigraphic distribution of the material discussed here, according to different geological subdivisions of the Upper Jurassic of the Lusitanian Basin. Re-drawn from Mateus et al. (2017).

The Microsoft Excel files used for mathematical estimates and calculations are given in the Supplemental material.

Institutional abbreviations

MAP, Museo Aragonés de Paleontología, Teruel, Spain; **MG**, Museu Geológico, Labóratorio Nacional de Energia e Geologia, Lisbon, Portugal; **ML**, Museu da Lourinhã, Lourinhã, Portugal; **MPA**, Museo Paleontológico de Alpuente, Alpuente, Spain; **OUMNH**, Oxford University Museum of Natural History, Oxford, UK; **RBINS**, Royal Belgian Institute of Natural Sciences, Brussels, Belgium; **SHN**, Sociedade de História Natural, Torres Vedras, Portugal; **USNM**, National Museum of Natural History, Smithsonian Institution, Washington, DC, USA.

Systematic palaeontology

Dinosauria Owen, 1842
Ornithischia Seeley, 1887 (*sensu* Madzia et al., 2021)
Ornithopoda Marsh, 1881 (*sensu* Madzia et al., 2021)
Iguanodontia Dollo, 1888 (*sensu* Madzia et al., 2021)
Dryomorpha Sereno, 1986 (*sensu* Madzia et al., 2021)
Ankylopollexia Sereno, 1986 (*sensu* Madzia et al., 2021)
Ankylopollexia indet.
(Figs 2–10)

Material. SHN.JJS.015, an associated skeleton consisting of a dorsal vertebra, left scapula, right humerus, right femur, right calcaneum. ML 434, an isolated left femur. SHN.JJS.073, an isolated right femur. ML 2055, an isolated right femur.

Occurrence. Upper Kimmeridgian–lowest Tithonian (Late Jurassic) of the Lusitanian Basin, Portugal. SHN.JJS.015, Praia da Corva, Praia da Amoreira-Porto Novo Formation/Porto Novo Member of the Lourinhã Formation, municipality of Torres Vedras. ML 434 (Praia do Caniçal), ML 2055 (Praia do Zimbral) and SHN.JJS.073 (Praia da Peralta) all come from the Sobral Formation/Praia Azul Mb of the Lourinhã Formation in the municipality of Lourinhã.

SHN.JJS.015

Dorsal vertebra

SHN.JJS.015 preserves one isolated posterior dorsal vertebra. The vertebra is complete, and the centrum and neural arch are fused together, suggesting osteological maturity for the individual (Maidment et al., 2022). This is consistent with what is known in other ornithopod taxa (Griffin et al., 2021), even though the timing of the fusion of neural sutures is quite variable within Reptilia. The distal ends of the neural spine and transverse processes are slightly eroded (Fig. 2). The neural canal is preserved but filled with matrix. The vertebra is robust and stout in general appearance, and the arrangement of the parapophysis/diapophysis suggests that it is located between the 11th and 13th position in the dorsal series. The centrum is stout and slightly amphicoelous (Fig. 2B,D), showing a strong concave ventral margin and a slight ventral keel (Fig. 2D). Several nutrient foramina are present in the lateral surface of the centrum (Fig. 2B). Although the centrum and the neural arch are fused, in lateral view a neurocentral suture is clearly visible and extends along the entire length of the centrum. On the anterior surface of the neural arch and immediately dorsal to the neural canal, two stout prezygapophyses are located; these are dorsolaterally oriented, with an angle greater than 115° between them. Two small laminae diverge from the neural spine to the two prezygapophyses. Immediately posterior to the lamina, on the two lateral surfaces, the transverse processes diverge dorsoposteriorly, forming an angle greater than 28° with the horizontal (Fig. 2A). The parapophyses are small and located ventrally to the diapophyses, which are rounded in section. On the posterior surface, the postzygapophyses originate at the base of the neural spine. Anteroventrally to the postzygapophyses, the posterior centrodiapophyseal lamina, the postzygodiapophyseal lamina and the centropostzygapophyseal lamina form two shallow depressions (Fig. 2C–C1). The transversely flattened neural spine is slightly arched posteriorly and is slender in proportions, and it is broken towards its apex. The neural spine is roughly twice as tall as the centrum.

Remarks. The preserved dorsal vertebra, located approximately in the middle/posterior part of the dorsal series, differs from those of *Uteodon aphanoecetes*, *Cumnoria prestwichii* and *Camptosaurus dispar* in having a strongly concave ventral margin (Carpenter & Galton, 2018; Carpenter & Wilson, 2008; Galton & Powell, 1980; Gilmore, 1909). None of the described dorsal vertebrae of *Cumnoria prestwichii* presents a strongly concave ventral margin in lateral view (Maidment et al., 2022, pl. 4). The same condition is seen in the holotype of *Uteodon aphanoecetes*, where the dorsal vertebrae D-4 to D-9 present an almost straight ventral margin that becomes slightly arched in D-14 to D-16 (Carpenter & Wilson, 2008, fig. 12). *Camptosaurus dispar* presents a condition very similar to *Uteodon aphanoecetes*, retaining relatively straight

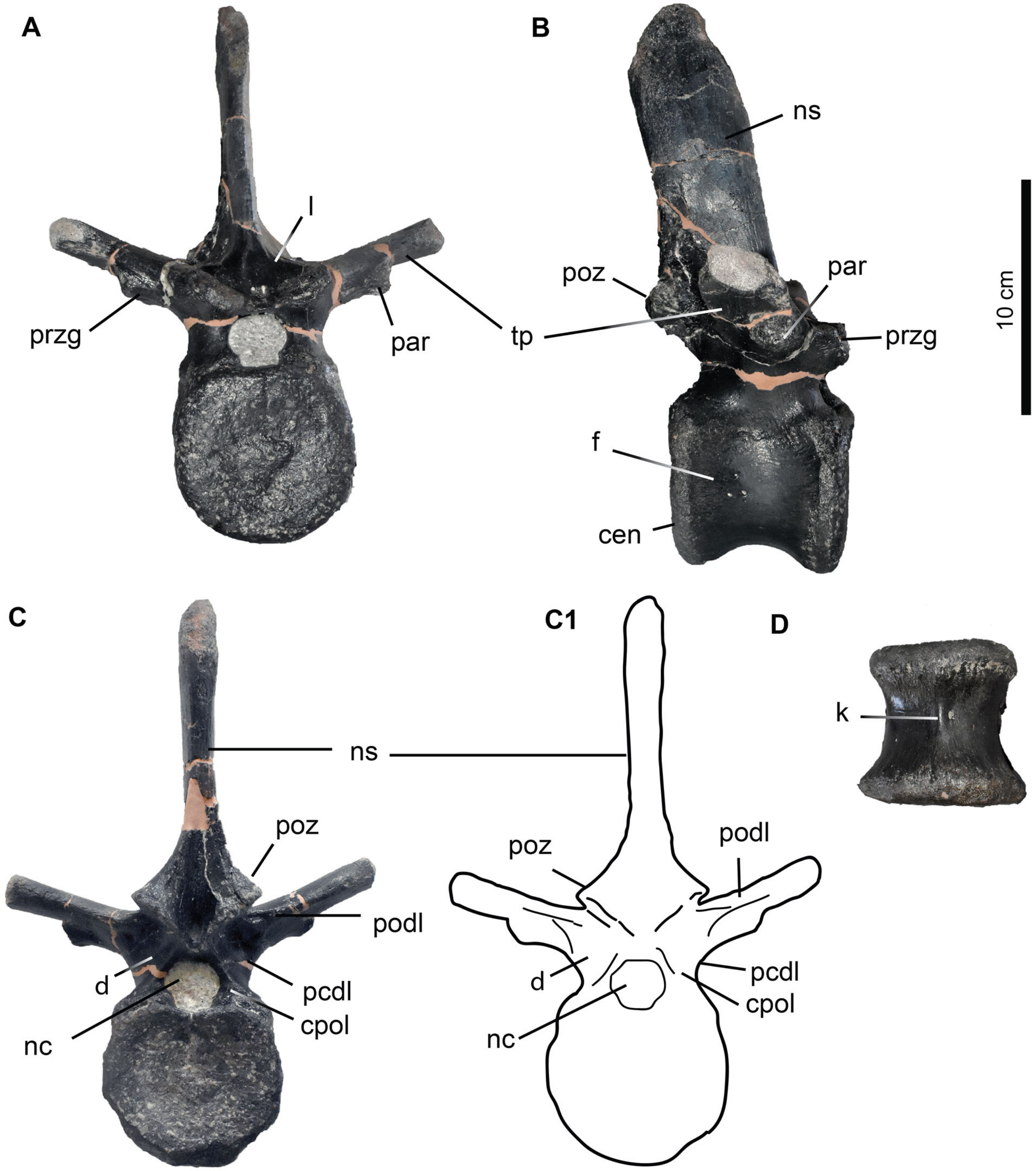

Figure 2. Indeterminate ankylopollexian SHN.JJS.015; **A**–**D** dorsal vertebra in anterior (**A**), right lateral (**B**), posterior (**C**–**C1**) and ventral (**D**) views; **E**–**H**, right calcaneum in medial (**E**), lateral (**F**) dorsal (**G**) and ventral (**H**) views; **Abbreviations**: **cen**, centrum; **cpol**, centropostzygapophyseal lamina; **d**, depression; **f**, foramina; **l**, lamina; **k**, keel; **nc**, neural canal; **ns**, neural spine; **par**, parapophysis; **pcdl**, posterior centrodiapophyseal lamina; **podl**, postzygodiapophyseal lamina; **poz**, postzygapophysis; **przg**: prezygapophysis; **tp**, transverse process.


A
ap
dr
df
sgf
em
gl
scl
B
mb
C
ap
ms
mb
gl
D
gl
mb
10 cm

ventral margins up to D-13 (Carpenter & Galton, 2018, fig. 22; Gilmore, 1909, fig. 16). On the other hand, the condition observed in the SHN.JJS.015 dorsal vertebra is more similar to the condition interpreted in *Brighstoneus simmondsi*, *Mantellisaurus atherfieldensis*, *Morelladon beltrani*, *Ouranosaurus nigeriensis* and *Iguanodon bernissartensis* (Bertozzo et al., 2017; Gasulla et al., 2015; Lockwood et al., 2021; Norman, 1980, 1986). The concavity of the ventral surface of the centrum is stronger than that of the isolated vertebrae described by Rotatori et al. (2020), although this may be due to differences related to the position along the vertebral column. In general, Late Jurassic iguanodontians seem to have a less arched margin of the ventral surface of the centrum than their Early Cretaceous counterparts, except for SHN.JJS.015. Other than this, the abovementioned features are typical of ankylopollexians (Norman, 2004). Compared with other Late Jurassic ankylopollexians, the SHN.JJS.015 posterior dorsal vertebra can be distinguished from those of *Cumnoria prestwichii* in having a weak ventral keel on its ventral side (Maidment et al., 2022). Furthermore, the preserved vertebra differs from other dorsal vertebrae located in the posterior portion of the series in not showing the usual anteroposterior compression seen in other taxa such as *Cumnoria prestwichii*, *Camptosaurus dispar* and *Uteodon aphanoecetes* (Carpenter & Galton, 2018; Carpenter & Wilson, 2008; Maidment et al., 2022).

Scapula

The left scapula of specimen SHN.JJS.015 is complete, although the specimen has undergone some superficial breakages, later restored with epoxy resin. The scapular blade is a straight, stout element and is slightly bent lateromedially (Fig. 3B). The dorsal and ventral margins are subparallel, diverging slightly in the thin distalmost portion (Fig. 3A). The proximal end of the scapula flares abruptly from the blade, its dorsal and ventral margins being strongly emarginated (Fig. 3A, C). The overall shape of the proximal end of the scapula is subtriangular, presenting a rugose lateral surface and an irregular surface of the proximal margin due to the presence of several blunt proximal processes. The acromion process is well developed and round, following the definition of McDonald (2011), forming a buttress that extends distally. The acromion process is the culmination of a deep emargination that constitutes the deltoid ridge (Fig. 3A). Ventral to the acromion, in the area corresponding to the coracoid suture, the proximal margin of the scapula projects slightly dorsally and forms a wavy surface (Fig. 3A). This latter surface, together with the base of the acromial buttress, bears a deep sulcus that extends parallel to the acromion and merges with a shallow deltoid fossa. In mediolateral view, the coracoid suture is an expanded sub-triangular surface, ventrally separated from the glenoid surface by a constriction. Here, a blunt eminence protrudes proximally, delimiting the supraglenoid fossa, which is a deeply excavated, cup-like depression. Notably, this blunt eminence slightly separates the supraglenoid from the deltoid fossa. The whole lateral surface of the proximal end of the scapula is a continuous depression. The dorsal margin of the supraglenoid fossa is the only interruption of this surface (Fig. 3A). Ventrally and medially to the supraglenoid fossa, the margin gently deflects into the glenoid, which in mediolateral view is reniform and mediolaterally expanded. The distal end of the scapular blade shows smooth dorsal and ventral margins that form its dorsal and ventral corners, respectively, the latter being posteroventrally expanded. Both corners of the distal end of the scapula are rounded, without any dorsal or ventral protrusions or processes. Despite a very small amount of breakage to the edge of the bone, we consider the general morphology to be genuine.

Remarks. The acromion in SHN.JJS.015 (Fig. 4A) is rounded and inclined as in *Uteodon aphanoecetes* (Fig. 4B) and dryosaurids, differing from the triangular acromion present in *Camptosaurus dispar* (Fig. 4B,D) (specimen USNM 4282, holotype of *Camptosaurus browni*) (Galton, 1981; Hübner, 2018; McDonald, 2011). Carpenter and Lamanna (2015) state that

> Carpenter and Wilson (2008, fig. 17) illustrated an array of acromial profiles in *Camptosaurus dispar*, including triangular, rounded, and truncated. As such, the shape of the acromial process cannot be used to distinguish *Camptosaurus dispar*, *Cumnoria prestwichii* (*sensu* McDonald 2011), and *Uteodon aphanoecetes* (*sensu* McDonald 2011), nor to separate the latter two taxa from the former.

In the figure in question, the authors represent the scapulae USNM 4282 and USNM 5473, both ascribed to *Camptosaurus dispar*. The two specimens differ from

◀

Figure 3. Indeterminate ankylopollexian SHN.JJS.015; left scapula in lateral (**A**), dorsal (**B**), medial (**C**) and ventral (**D**) views. **Abbreviations**: **ap**, acromion process; **df**, deltoid fossa; **dr**, deltoid ridge; **em**, eminence; **gl**, glenoid; **mb**, medial buttress; **ms**, muscular scar; **scl**, scapular labrum; **sgf**, supraglenoid fossa.

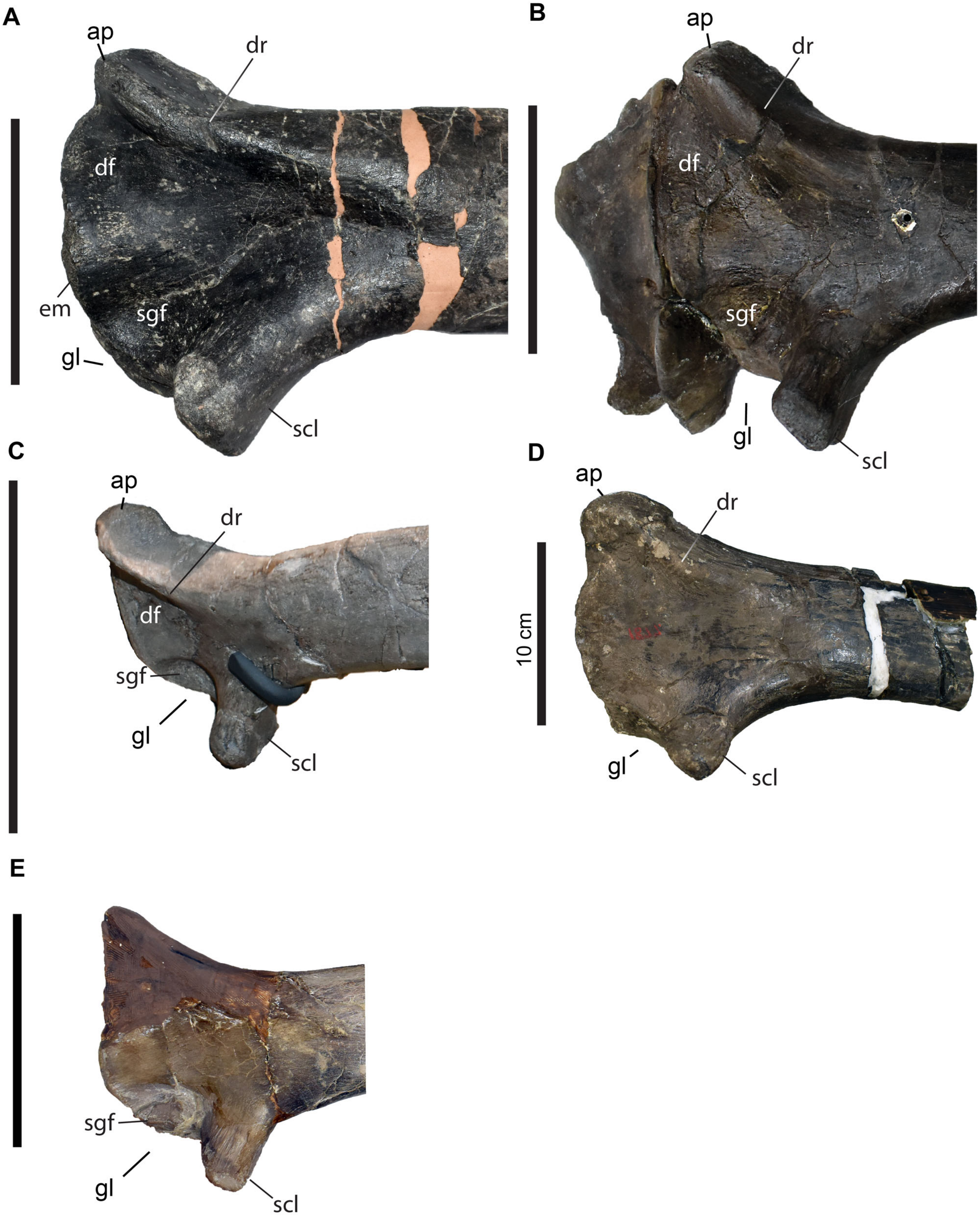

Figure 4. Comparative table of the proximal end of the scapula of selected ankylopollexian iguanodontian dinosaurs in lateral view. SHN.JJS.015 (**A**); *Camptosaurus dispar* (USNM 4282, *Camptosaurus browni* holotype) (**B**); *Uteodon aphanoecetes* holotype (CM 11337) (**C**); *Camptosaurus dispar* holotype (YPM 1887) (**D**); *Cumnoria prestwichii* holotype (OUMNH J.3303) reversed (**E**). **Abbreviations**: **ap**, acromion process; **df**, deltoid fossa; **dr**, deltoid ridge; **em**, eminence; **gl**, glenoid; **scl**, scapular labrum; **sgf**, supraglenoid fossa.


A
da
dm
sb
va
B
sb
C
?da
dm
sb
?va
D
da
dm
sb
va
10 cm

one another not just in the shape of the acromion process, but also in the bending of the scapular blade, a character that the authors use to differentiate *Camptosaurus dispar* from *Uteodon aphanoecetes*. To refer these specimens to the same taxon and imply intraspecific variation thus does not seem consistent with the argument made by the authors. The acromion of *Cumnoria prestwichii* is not preserved (Carpenter & Lamanna, 2015; Galton & Powell, 1980; Maidment et al., 2022). Another specimen from Praia da Peralta, ML 2042, shares with SHN.JJS.015 the rounded shape of the acromion (Rotatori et al., 2020, fig. 8). Early Cretaceous styracosternans such as *Mantellisaurus atherfieldensis*, *Iguanodon bernissartensis*, *Ouranosaurus nigeriensis*, *Hypselospinus fittoni* and *Altirhinus kurzanovi* show a rounded acromion process tapering dorsally, with an angle of approximately 90° with respect to the scapula (Bertozzo et al., 2017; Norman, 1980, 1986, 1998, 2015). The proximal end of the SHN.JJS.015 scapula is strongly emarginated, as in *Uteodon aphanoecetes* and *Camptosaurus dispar*, unlike that of ML 2042 (Carpenter & Galton, 2018; Carpenter & Wilson, 2008; Gilmore, 1909; McDonald, 2011; Rotatori et al., 2020). Moreover, SHN.JJS.015 differs from *Camptosaurus dispar* and *Uteodon aphanoecetes* in possessing a blunt process separating the deltoid from the supraglenoid fossa (Fig. 4A–D) (Carpenter & Galton, 2018; Carpenter & Wilson, 2008; Gilmore, 1909; McDonald, 2011). The scapular blade of SHN.JJS.015 is straight, as in *Camptosaurus dispar*, unlike ML 2042, *Uteodon aphanoecetes*, *Cumnoria prestwichii*, dryosaurids and most styracosternans (Fig. 5) (Carpenter & Galton, 2018; Carpenter & Wilson, 2008; Galton, 1981; Gilmore, 1909; Hübner, 2018; McDonald, 2011; Norman, 2004; Rotatori et al., 2020). A great difference in size between *Uteodon aphanoecetes* and *Cumnoria prestwichii* can be discerned (Fig. 5), the former being 67% (290 mm, see Gilmore 1925) and the latter 81% (352 mm, see Maidment et al., 2022) of the size of SHN.JJS.015. To assign SHN.JJS.015 to *Uteodon aphanoecetes* or to *Cumnoria prestwichii* would imply that the holotypes in question (CM 11337, OUMNH J.3303) represent younger individuals of the same taxon, indicating that the scapular blade becomes progressively straighter from a dorsoventrally arched condition. This is not consistent with what is known of the ontogenetic development of the closely related *Dysalotosaurus lettowvorbecki*, which retains this dorsoventral arching throughout its ontogenetic development (Hübner, 2018). This is also supported by Poole (2023), who considered the impact of ontogenetically variable characters on iguanodontian phylogenies and found no variation in the arching of the scapular blade (Fig. 5). The distal end of the specimen SHN.JJS.015 blade has rounded dorsal and ventral margins, lacking the hook-like processes of *Camptosaurus dispar* or the pointy edges of *Uteodon aphanoecetes* and more early-branching iguanodontians (Carpenter & Galton, 2018; Carpenter & Wilson, 2008; Hübner, 2018). Despite a slight degree of erosion, as noted above, the margin is complete, and no significant amount of bone is missing. Furthermore, the ratio between the maximum width of the scapular blade at its distal end and the maximum constriction of the scapular blade in lateral view (Mwsb/csb) (Verdú et al., 2017) appears to differ among the specimens: in SHN.JJS.015 the ratio is 1.32; in *Uteodon aphanoecetes* (CM 11337) it is 2.7; in *Cumnoria prestwichii* (OUMNH J.3303) it is 1.53; and in *Camptosaurus dispar* (USNM 4282, holotype of '*C. browni*') it is 2.57. Verdú et al. (2017) estimated the variability in the Mwsb/csb ratio within an *Iguanodon bernissartensis* population and found a range of 1.1–1.38, with a difference of 0.2 between the lower and higher values. The difference between SHN.JJS.015 and the other species under consideration here is greater, and only the holotype of *Cumnoria prestwichii* (OUMNH J.3303) approaches a value close to that range. The calculation that yielded these estimates is given in the Supplemental material.

Humerus

The right humerus of SHN.JJS.015 is broken at midshaft, and some parts of the diaphysis are lost. However, the preserved specimen is not morphologically deformed by taphonomic processes, allowing a clear assessment of the characters present therein. The specimen is a compact yet slender element, slightly sigmoidal in overall shape. On the proximal epiphysis, the humeral head is a stout process directed posterolaterally (Fig. 6C). The lateral tuberosity is a rounded and stout element, developing from the base of the humeral head (Fig. 6); it does not extend much anteriorly, and it is separated from the humeral head by a deep sulcus. The medial tuberosity projects medially without any inflection. It is important to note that both the lateral and medial tuberosities form an approximately straight

◄

Figure 5. Comparative table of scapular blade in lateral view of selected ankylopollexian iguanodontian dinosaurs. SHN.JJS.015 (**A**); *Camptosaurus dispar* (USNM 4282, *Camptosaurus browni* holotype) (**B**); *Cumnoria prestwichii* holotype (OUMNH J.3303) reversed (**C**); *Uteodon aphanoecetes* holotype (CM 11337) (**D**). **Abbreviations**: **da**, dorsal angle; **dm**, distal margin; **sb**, scapular blade; **va**, ventral angle.

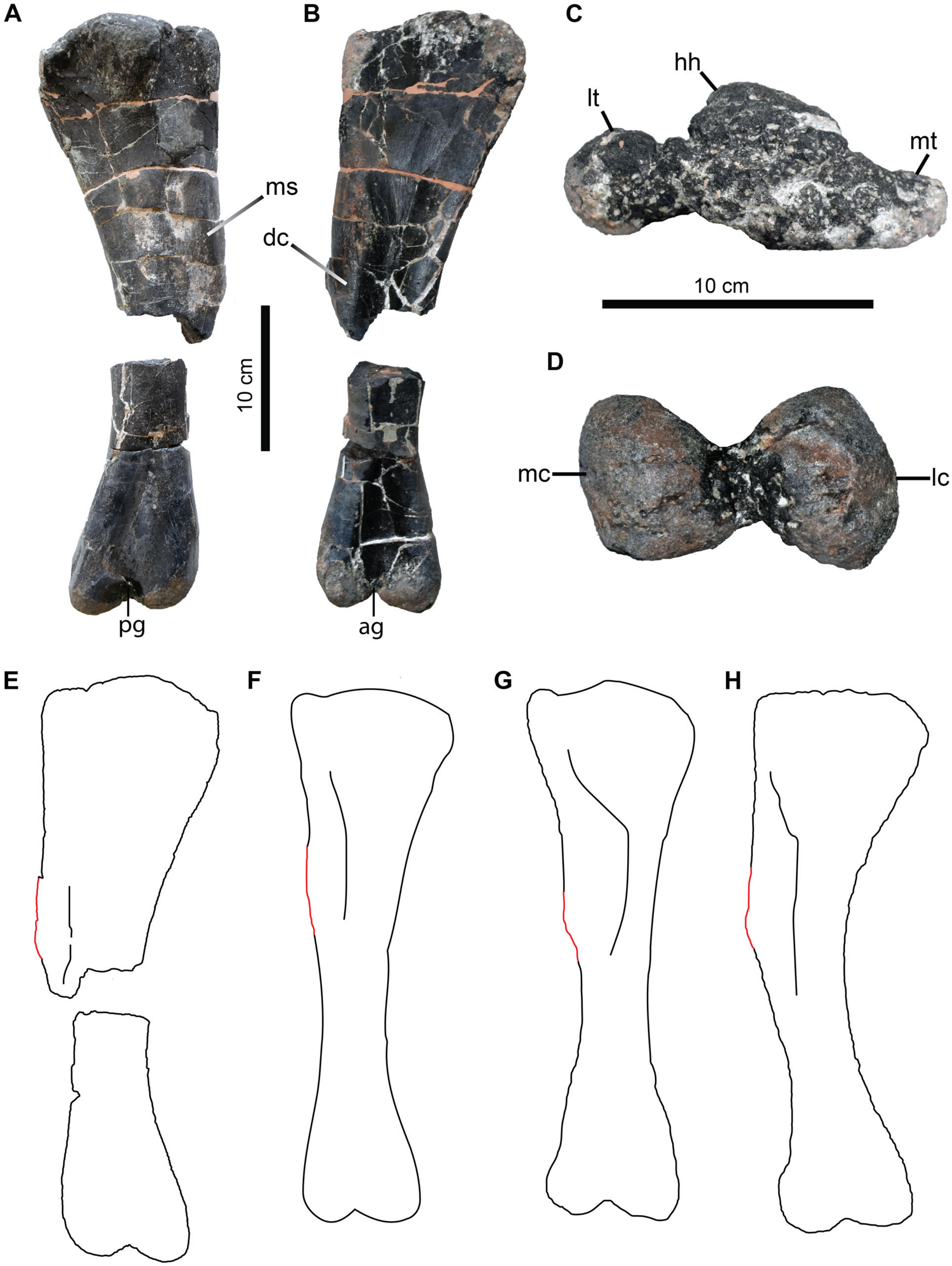
A
B
C
hh
lt
mt
ms
dc
10 cm
10 cm
D
mc
lc
pg
ag
E
F
G
H

angle, which we here define as ‘planar’, with respect to the humeral head. At the level of the mid-shaft, a low and scarcely developed deltopectoral crest is located at the anterolateral border (Fig. 6B). On the distal epiphysis, the medial and lateral condyles are subequal and rounded in shape, separated anteriorly and posteriorly by two deep grooves.

Remarks. The general proportions of the humerus are similar to those of other Jurassic ankylopollexians such as *Uteodon aphanoecetes* and *Cumnoria prestwichii* (Carpenter & Wilson, 2008; Galton & Powell, 1980), yet differing from the stout condition seen in the humerus of *Camptosaurus dispar* (Fig. 6E–H) (Carpenter & Galton, 2018; Gilmore, 1909). In comparison with Early Cretaceous styracosternans, the proportions of SHN.JJS.015 are closer to those of *Ouranosaurus nigeriensis* and RBINS 1551 (*Mantellisaurus atherfieldensis*) than to those of *Magnamanus soriaensis* or *Iguanodon bernissartensis* (Bertozzo et al., 2017; Norman, 1980, 1986, 2004; Verdú et al., 2017; Vidarte et al., 2016). The humeral shaft of SHN.JJS.015 is bent at mid-shaft, differing in this from *Uteodon aphanoecetes* and the specimen USNM 5473 (Fig. 6E–G) referred to *Camptosaurus dispar* (Carpenter & Wilson, 2008). However, specimen USNM 4282, likewise referred to *Camptosaurus dispar* (once the holotype of *Camptosaurus browni*; Gilmore, 1909), has the same angle at mid-shaft as SHN.JJS.015 (Fig. 6E,H). Similarly, the deltopectoral crest has a low rounded shape, as in *Uteodon aphanoecetes*, *Cumnoria prestwichii*, *Ouranosaurus nigeriensis* and other styracosternans, differing from the high and angled structure present in *Camptosaurus dispar* (USNM 5473, USNM 4282; Fig. 6E–H) (Carpenter & Galton, 2018; Carpenter & Wilson, 2008; Galton & Powell, 1980; Gilmore, 1909; Norman, 2004; Verdú et al., 2017). The posterolateral inflection of the humeral head is shared solely with *Uteodon aphanoecetes* (Carpenter & Wilson, 2008), a condition absent in other ankylopollexians (Bertozzo et al., 2017; Norman, 1980, 1986). Furthermore, the planar orientation of both the lateral and medial tuberosities with respect to the humeral head is shared only with *Cumnoria prestwichii* and differs from *Uteodon aphanoecetes* and *Camptosaurus dispar* (Carpenter & Galton, 2018; Carpenter & Wilson, 2008).

Femur

The right femur of specimen SHN.JJS.015 (Fig. 7 A–D) is complete, and both the proximal and distal ends are slightly eroded, without this compromising their shape and morphology (Fig. 7A–D). The femur appears to have undergone a high degree of distortion, as is particularly evident at the level of the distal epiphysis, since its anteroposterior axis is strongly tilted mediolaterally. The pressure that produced this high degree of distortion also provoked the collapse of most of the medial surface of the femoral shaft. Despite these alterations, the anatomical characters present in SHN.JJS.015 are well distinguishable and remain almost unchanged (Fig. 7A–D). The femoral shaft of SHN.JJS.015 is strongly bowed anteroposteriorly, although the proximal half of the shaft is straight (Fig. 7A–D). The deflection point occurs immediately distal to the fourth trochanter. In anterior view, the femoral shaft does not bow strongly medially. Proximally, the lesser trochanter is lower in height than the greater trochanter, and there is no space between these two elements. The lateral surface of the greater trochanter is concave, and it is separated from the wide femoral head by a small constriction. The head of the femur is inclined about 30° proximally (Fig. 7A–D). A deep scar is present on the posterior surface of the femoral head. Distally, the fourth trochanter is pendant-like, and its base is located towards the midline of the shaft. The collapse in the medial portion of the surface of the diaphysis hampers any attempt to assess the shape and position of the scar for the insertion of the *Musculus caudofemoralis longus* in SHN.JJS.015. The distal epiphysis shows a partially enclosed flexor groove in SHN.JJS.015, whereas the extensor groove remains fully open. The medial condyle of the femur is a stout element, possessing a slightly convex medial margin, and it is separated from the lateral condyle by a U-shaped extensor intercondylar groove. Despite the degree of distortion of the specimen, on the anterior surface of the femoral shaft a crest extends proximally from the medial condyle to the lesser trochanter. The lateral condyle is well developed anteriorly and possesses a conspicuous finger-like posterior process. In lateral view, the medial condyle appears strongly developed anteroposteriorly, passing beyond the posterior process of the lateral condyle (condylid).

◀

Figure 6. Indeterminate ankylopollexian SHN.JJS.015; **A**–**D**, right humerus in posterior (**A**), anterior (**B**), proximal (**C**) and distal (**D**) views. Interpretative drawings of selected ankylopollexian iguanodontian dinosaur humeri in anterior view: SHN.JJS.015 (**E**), *Uteodon aphanoecetes* holotype (CM 11337) (**F**), *Camptosaurus dispar* USNM 5437 (**G**), USNM 4282 (**H**). **Abbreviations**: **ag**, anterior groove; **dc**, deltopectoral crest; **hh**, humeral head; **lc**, lateral condyle; **lt**, lateral tuberosity; **mc**, medial condyle; **ms**, muscular scar; **mt**, medial tuberosity; **pg**, posterior groove.

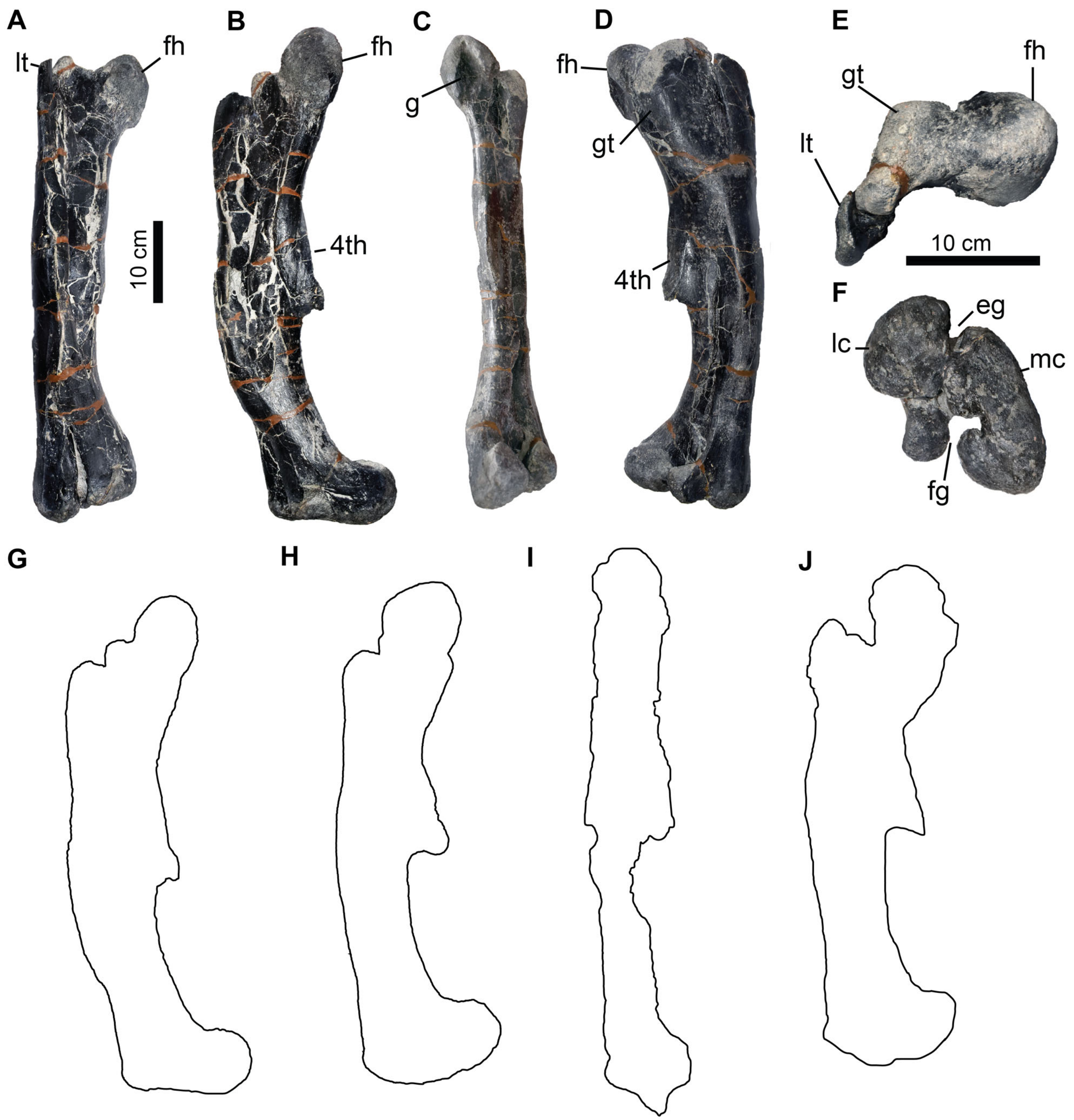

Figure 7. Indeterminate ankylopollexian SHN.JJS.015; **A**–**D**, right femur in anterior (**A**), medial (**B**), posterior (**C**), lateral (**D**), proximal (**E**) and distal (**F**) views. Interpretative drawings of selected ankylopollexian femora in medial view: (**G**) SHN.JJS.015, (**H**) *Camptosaurus dispar* (USNM 5818), (**I**) *Oblitosaurus bunnueli* (MAP-8290) and (**J**) *Uteodon aphanoecetes* holotype (CM 11337). **Abbreviations**: **4th**, fourth trochanter; **eg**, extensor groove; **fg**, flexor groove; **fh**, femoral head; **g**, groove; **gt**, greater trochanter; **lc**, lateral condyle; **lt**, lesser trochanter; **mc**, medial condyle.

Remarks. The femur of SHN.JJS.015 exhibits the condition observed among early-diverging iguanodontians of being strongly bowed anteroposteriorly, contrasting with the straight femoral shafts of derived styracosternans, i.e. hadrosauriforms (Norman, 2004). This plesiomorphic condition is also present in the ankylopollexians *Camptosaurus dispar*, *Uteodon aphanoecetes*, *Cumnoria prestwichii*, *Draconyx loureiroi* and

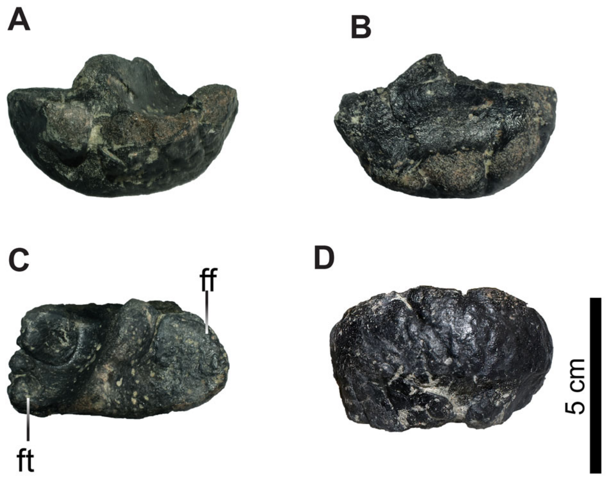

Figure 8. Indeterminate ankylopollexian SHN.JJS.015, right calcaneum **A**–**D** in medial (**A**), lateral (**B**), dorsal (**C**) and ventral (**D**) views. **Abbreviations**: **ff**, facet for fibula; **ft**, facet for tibia.

Oblitosaurus bunnueli (Carpenter & Wilson, 2008; Galton & Powell, 1980; Gilmore, 1909; Rotatori et al., 2022; Sánchez-Fenollosa et al., 2023). Another early-diverging condition present in the femur of SHN.JJS.015 is the blade-like but slightly pendant fourth trochanter, which is common in neornithischians and dryosaurids and found in *Camptosaurus dispar*, *Uteodon aphanoecetes* and *Oblitosaurus bunnueli* (Carpenter & Galton, 2018; Dieudonné et al., 2020; Galton, 1981; Gilmore, 1909; Hübner, 2018; McDonald, 2011; Sánchez-Fenollosa et al., 2023). As in other ankylopollexians, the base of the fourth trochanter is located towards the mid-shaft (Norman, 2004). The well-demarcated ridge present on the anterior surface of the shaft, extending from the medial condyle dorsally to the lesser trochanter, is a feature common in Iguanodontia, with *Draconyx loureiroi* being the only exception (Norman, 2004; Rotatori et al., 2022). The separation of the medial and lateral condyles by an open U-shaped extensor groove is a condition shared with *Valdosaurus*

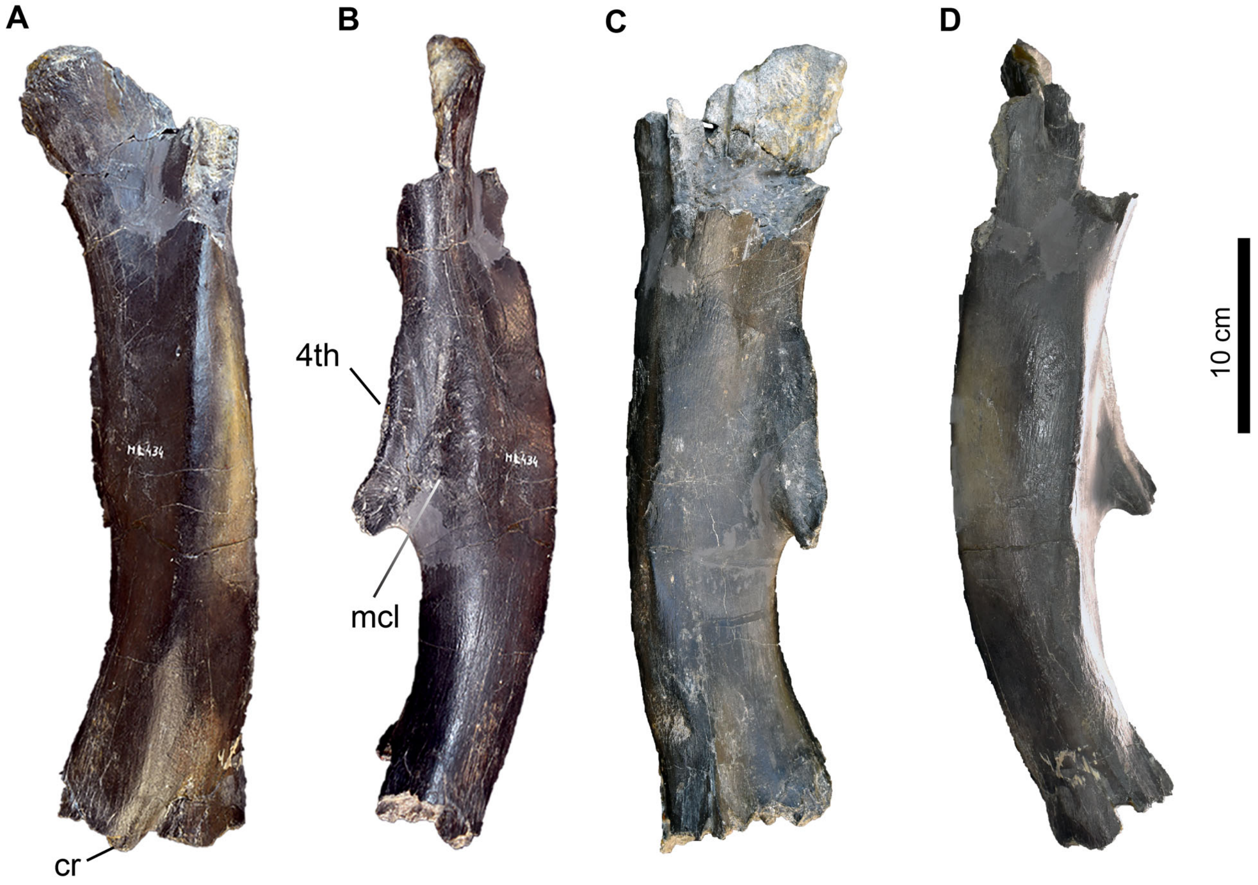

Figure 9. Indeterminate ankylopollexian ML 434, left femur **A**–**D** in anterior (**A**), medial (**B**), posterior (**C**) and lateral (**D**) views. **Abbreviations**: **4th**, fourth trochanter; **cr**, crest; **mcl**, *Musculus caudofemoralis longus* scar.

Figure 10. Indeterminate ankylopollexian ML 2055, right femur **A**–**F,** in anterior (**A**), medial (**B**), posterior (**C**), lateral (**D**), proximal (**E**) and distal (**F**) views; SHN.JJS.073, right femur **G**–**N**, in anterior (**G**), medial (**J**), posterior (**K**), lateral (**L**), proximal (**M**) and distal (**N**) views. **Abbreviations**: **4th**, fourth trochanter; **cod**, condylid; **cr**, crest; **eg**, extensor groove; **fg**, flexor groove; **gt**, greater trochanter; **lc**, lateral condyle; **mc**, medial condyle; **mcl**, *Musculus caudofemoralis longus* scar.

canaliculatus, *Camptosaurus dispar*, *Uteodon aphanoecetes*, *Cumnoria prestwichii*, *Draconyx loureiroi* and *Oblitosaurus bunnueli* (Barrett et al., 2011; Carpenter & Wilson, 2008; Galton & Powell, 1980; Gilmore, 1909; Rotatori et al., 2022; Sánchez-Fenollosa et al., 2023), differing clearly from Early Cretaceous styracosternans (Norman, 2004). The slight overhang of the medial condyle over the flexor groove present in SHN.JJS.015 is a common feature of large-sized ankylopollexians (Norman, 2004), differing from the Iberian taxa *Draconyx loureiroi* and *Oblitosaurus bunnueli* (Rotatori et al., 2022; Sánchez-Fenollosa et al., 2023). The posterior development of the medial condyle is shared solely with *Uteodon aphanoecetes*, differing from coeval and sympatric ankylopollexian taxa (Carpenter & Galton, 2018; Carpenter & Wilson, 2008; Rotatori et al., 2022; Sánchez-Fenollosa et al., 2023).

Calcaneum

The right calcaneum of SHN.JJS.015 is complete and unaltered; it has undergone a low degree of erosion in some parts of the edges. In mediolateral view, the calcaneum is hemispherical, and a dorsally prominent (anteromedially) diagonal ridge separates the articular facet of the tibia from the facet for the fibula on its dorsal surface (Fig. 8C). The two articular facets are located on two different levels; the facet for the fibula is located more ventrally than the tibial facet (Fig. 8C). The articular facet for the tibia is more deeply excavated than the one for the fibula. The lateral surface of the calcaneum is flat. The ventral surface of the calcaneum is rounded and smooth.

Remarks. The calcaneum does not differ from the general anatomy of ankylopollexians (Norman, 2004), including Jurassic ankylopollexian taxa such as *Draconyx loureiroi*, *Camptosaurus dispar*, *Cumnoria prestwichii*, *Oblitosaurus bunnueli* and *Uteodon aphanoecetes*.

In addition to SHN.JJS.015, three additional specimens have been recovered that are attributable to Ankylopollexia indet. The lack of diagnostic characters and the scarcity of overlapping material (see discussion below) hinder both the erection of a new taxon and the attribution of all the material to the same taxon.

ML 434

Femur

The left femur ML 434 was reported by Mateus and Antunes (2001) and assigned to *Draconyx loureiroi.* However, Rotatori et al. (2022) have since shown that *Draconyx loureiroi* and this specimen differ in several respects and that ML 434 in fact shares more features with SHN.JJS.015. For a more thorough and detailed description of ML 434, we refer the reader to the original description by Mateus and Antunes (2001) and the reassessment by Rotatori et al. (2022). Here we focus more on a comparison of the common features shared with SHN.JJS.015.

Remarks. ML 434, like SHN.JJS.015 and other iguanodontians with the exception of *Draconyx loureiroi*, possesses a high crest on the anterior surface (Fig. 9A) of the shaft running dorsally from the medial condyle up to the lesser trochanter (Norman, 2004; Rotatori et al., 2022). As in SHN.JJS.015, a pendant fourth trochanter is highly developed, and its base reaches the mid-shaft, a condition shared with early-diverging iguanodontians (Fig. 9B), *Camptosaurus dispar* and *Uteodon aphanoecetes*. Like SHN.JJS.015, the insertion scar for the *Musculus caudofemoralis longus* is attached to the base of the trochanter, a feature shared with other ankylopollexians (Norman, 2004).

ML 2055

Specimen ML 2055 has already been reported and described by Rotatori et al. (2020) and ascribed to the clade Dryosauridae, although the authors recognized that a juvenile ankylopollexian interpretation was still probable. Comparison with other material presented in this contribution supports the second hypothesis.

Femur

For a more thorough general overview of the femur ML 2055, we refer the reader to the original description by Rotatori et al. (2020). Here we focus on the anatomical traits that have been wrongly assessed. Rotatori et al. (2020) described the femoral shaft of ML 2055 as robust in general proportions and strongly bent anteroposteriorly (Fig. 10B). Although the shaft can be considered genuinely bent, this bending is not homogeneously distributed across the entire shaft. Instead, the proximal half of the shaft is straight, and the shaft abruptly deflects posteriorly ventral to the fourth trochanter (Fig. 10B). The fourth trochanter is blade-like, and the base is clearly located at the mid-shaft, contrary to what was reported by Rotatori et al. (2020). This mistake was induced by the fact that the proximal epiphysis is broken and was restored with epoxy, but it was misplaced proximomedially (Fig. 10B). Moreover, Rotatori et al. (2020) did not correctly assess the amount of missing bone on the proximal epiphysis, and this further affected the interpretation of the position of the base of this structure (Fig. 10A–D). The fourth trochanter, despite its proximal eminent crest being slightly eroded, is blade-like and extensively developed proximoposteriorly, possessing a higher proximal margin. The state of preservation prevented Rotatori et al. (2020) from recognizing a high crest running from the medial condyle on the medial surface up to the lesser trochanter. The anterolateral margin of the lateral condyle is rounded, and it is stout in its general proportions (Fig. 10F). The medial margin of the medial condyle is straight, as Rotatori et al. (2020) already noted.

Tibia

Regarding the tibia, we have no particular remarks on ML 2055 with respect to the original description by Rotatori et al. (2020).

SHN.JJS.073

Femur

The right femur SHN.JJS.073 is a complete and isolated specimen. It underwent breakage at the level of the proximal epiphysis and the distal epiphysis, lacking proximally part of the lesser trochanter and distally the posterior process of the lateral condyle (Fig. 10J). The specimen is bowed anteroposteriorly, but this curvature is not homogeneous across the shaft. In fact, the proximal half of the femoral shaft is straight, whereas the distal half deflects abruptly posteriorly (Fig. 10J). The proximal epiphysis preserves the femoral head, but the fracture obliterated the proximalmost part of the lesser trochanter (Fig. 10J). The femoral head is separated from the greater trochanter by a constriction, although the intertrochanteric groove is relatively shallow (Fig. 10M). The lateral surface of the greater trochanter is rounded. Distal to the femoral head, the greater trochanter and the preserved base of the lesser trochanter are not separated or arranged in a divergent fashion. A blade-like, moderately high fourth trochanter extends from the proximal half of the shaft, and its base reaches its middle (Fig. 10J). Medial to the fourth trochanter and contacting its margin, the deep scar for the insertion of the *Musculus caudofemoralis longus* extends parallel to the trochanter. The fourth trochanter and the insertion scar have the same proximodistal extension along the shaft (Fig. 10K). The distal epiphysis presents open flexor and extensor grooves (Fig. 10N). The extensor groove is U-shaped in section and extends proximally, not being extremely deep (Fig. 10N). The medial condyle has a rounded anterior margin, which becomes progressively straighter on the medial surface (Fig. 10N). The posterior process of the medial condyle does not extend far posteriorly and does not overhang the flexor groove. The preserved lateral condyle has a smooth and rounded anterior margin and is substantially smaller than the medial one (Fig. 10N).

Remarks. ML 2055 and SHN.JJS.073 are similar in dimensions and proportions. They share the following features: a bowed femoral shaft, resulting from the inflection of the distal half with respect to the proximal half; a low, blade-like fourth trochanter located proximally but the base of which reaches the mid-shaft; the insertion scar of the *Musculus caudofemoralis longus* located at the base of fourth trochanter. This combination of characters is consistent with a juvenile ankylopollexian *bauplan*, more than with dryosaurids or other early-diverging ornithopods (Dieudonné et al., 2020; Horner et al., 2009; Hübner, 2018). The location of the general bending of the shaft and that of the fourth trochanter in early-diverging iguanodontians have been shown to undergo severe transformation during ontogeny (Hübner, 2018), which is consistent with the observations made here. The specimens under discussion share the crest present on the anterior surface of the shaft with most iguanodontians, including SHN.JJS.015 and ML 434, but not with *Draconyx loureiroi* (Dieudonné et al., 2020; Norman, 2004; Rotatori et al., 2022). The flexor groove of ML 2055 is open like that of *Draconyx loureiroi*, although they differ in shape (Rotatori et al., 2022). ML 2055 and SHN.JJS.073 preserve a combination of characters that is consistent with juvenile ankylopollexians: extremely reduced size, together with synapomorphies of the clade that rule out attribution to any other group (Fig. 6) (Dieudonné et al., 2020; Horner et al., 2009; Hübner, 2018). Indeed, in ontogenetic trajectories of ornithischian dinosaurs, long bones come close to showing an isometric growth pattern (Kilbourne & Makovicky, 2010). For this reason, ontogenetic stages in iguanodontians are defined by histological features (Hübner, 2012), with unclear osteological correlates. We therefore conservatively refer to the individuals represented by smaller femora in the sample as ‘juveniles’, although their histological characterization is currently ongoing. Whatever the case, we can note some macroscopic features. For instance, the location of the general bending of the shaft and that of the fourth trochanter have been shown not to undergo a marked transformation during ontogeny in *Dysalotosaurus lettowvorbecki* (Hübner, 2018), which is consistent with what has been noted here. However, in the Cretaceous styracosternans these structures actually seem to range from the described plesiomorphic condition to the apomorphic state of Styracosterna (Verdú et al., 2015). The only marked differences are the size of the fourth trochanter and its protrusion, which is slightly pendant in ML 434 and SHN.JJS.015.

Phylogenetic analysis

The phylogenetic analysis returned four most-parsimonious trees of 459 steps (consistency index = 0.545, retention index = 0.839, rescaled consistency index = 0.457). The overall topology (Fig. 11) of the consensus of the four trees generally agrees with previous analyses of this data set (Lockwood et al., 2021; Rotatori et al.,

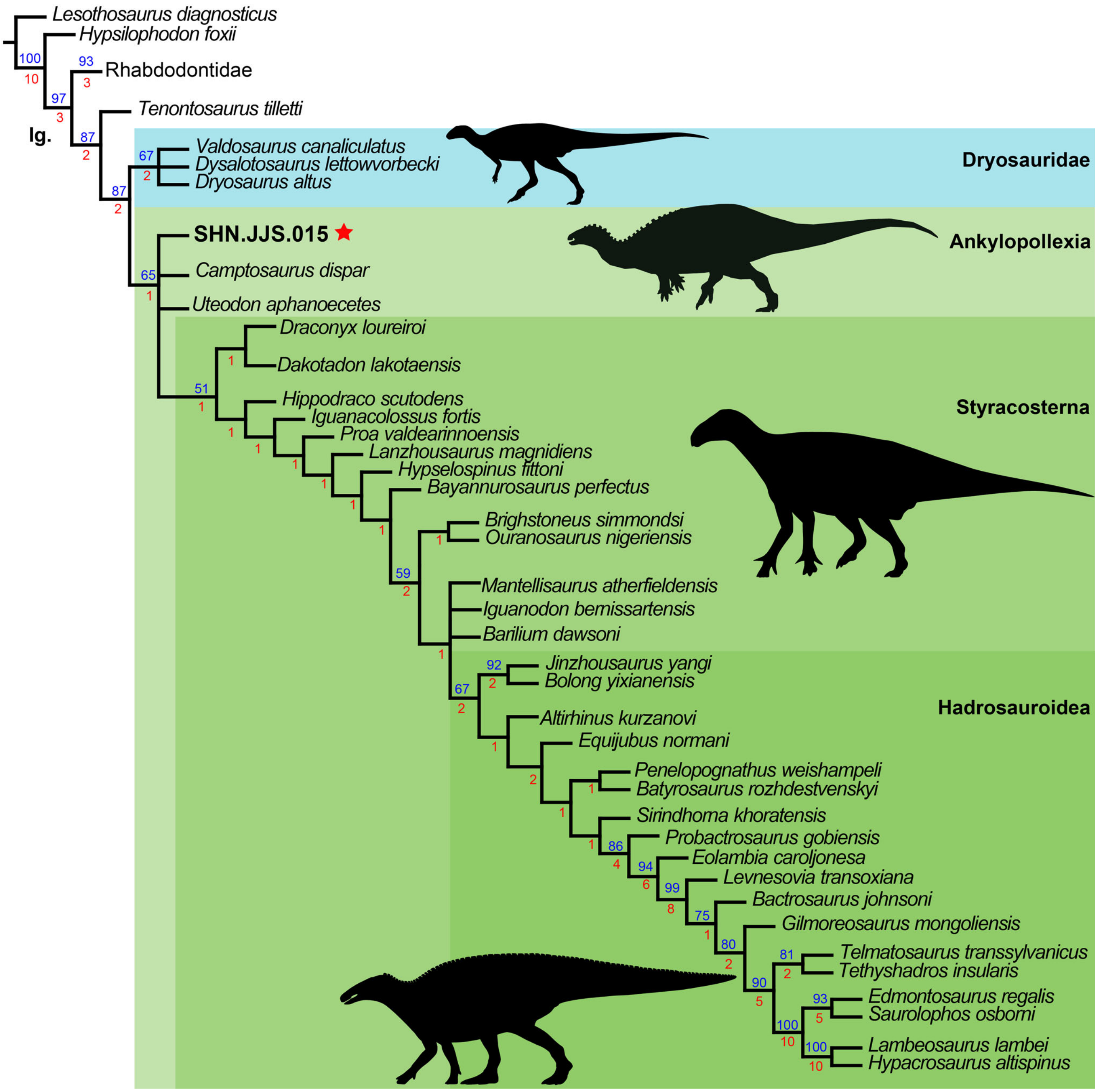

Figure 11. Strict consensus tree of two most-parsimonious trees recovered by the analysis, showing the affinities of SHN.JJS.015. Ig. represents the clade Iguanodontia. The numbers above branches (in blue) represent bootstrap values, whereas the the numbers below branches (in red) represent Bremer support values. Silhouettes from http://phylopic.org/. Credit: Tasman Dixon, Matthew Dempsey, used with permission under CC BY 4.0/CC0 01 license.

2022; Xu et al., 2018). However, we note some significant differences: *Brighstoneus simmondsi* is recovered as a sister taxon to *Ouranosaurus nigeriensis*, within a sister clade to other hadrosauriforms. The base of this latter clade is less resolved than in other analyses, with *Iguanodon bernissartensis*, *Mantellisaurus atherfieldensis* and *Barilium dawsoni* found in a polytomy with more deeply nested taxa. SHN.JJS.015 is recovered at the base of Ankylopollexia in a polytomy with *Camptosaurus dispar*, *Uteodon aphanoecetes* and Styracosterna, based on the unambiguous synapomorphy of a U-shaped extensor intercondylar groove (char. 118:1). Other characters that support the inclusion of SHN.JJS.015 in Ankylopollexia include the fourth trochanter arising at the dorsoventral midpoint of the femoral shaft (char. 117:1).

Mass and body length estimation

SHN.JJS.015 is estimated to be 1378 kg in weight, whereas ML 434 weighs 408 kg, and the smallest specimens (SHN.JJS.073 and ML 2055) weigh 112 kg and 99 kg, respectively.

Furthermore, the body length estimation for SHN.JJS.015 returned values of 4.5 m (subcursorial model) and 5 m (cursorial model) (see Supplemental material). The individual represented by ML 434 is estimated to have been 3.6 (cursorial model) or 3.1 (subcursorial model) metres in length, whereas ML 2055 and SHN.JJS.073 are estimated by both models to have been approximately >2 m in length, without much difference between the two of them.

Discussion

Systematic affinities

SHN.JJS.015 is recovered as one of the earliest-diverging forms of Ankylopollexia based on the unambiguous synapomorphy of the U-shaped extensor intercondylar groove. Further characters in common with other ankylopollexians include the fourth trochanter located at mid-shaft and a scar for the insertion of the *Musculus caudofemoralis longus* that contacts the base of the fourth trochanter. The pendant, blade-like fourth trochanter, as indicated above, is shared with some other coeval taxa such as *Camptosaurus dispar* and *Uteodon aphanoecetes* (Carpenter & Galton, 2018; Galton & Powell, 1980). The scapula and humerus present a unique combination of characters that indicates a complex evolutionary history for this group. The scapula presents a rounded acromion process as in *Uteodon aphanoecetes*, but the straight scapular shaft resembles the condition of *Camptosaurus dispar* (Carpenter & Galton, 2018; Carpenter & Wilson, 2008). In turn, the absence of any hook-like or pointy process on the distal end of the scapula clearly distinguishes SHN.JJS.015 from the abovementioned taxa (Carpenter & Galton, 2018; Carpenter & Wilson, 2008; Gilmore, 1909). Furthermore, the Mwsb/csb ratio in the scapula clearly differentiates SHN.JJS.015 from other coeval taxa. Carpenter and Lamanna (2015) argue that specimens ascribed to *Camptosaurus dispar* show various character states regarding the scapular blade, implying a high degree of intraspecific variability for this anatomical feature. However, this assumes that all the specimens of large-sized ankylopollexians recovered from Quarry 13 in the YPM and USNM collections represent a single taxon. Gilmore (1909) noted some significant differences among the specimens recovered, although he subsequently reconsidered his conclusions (Gilmore, 1925). Galton and Powell (1980) synonymized all the putative species of *Camptosaurus* with the species *Camptosaurus dispar*, but did not offer a clear discussion of what characters are considered variable within species, stating generically that "given the range of individual variation shown by two species of *Dryosaurus*, and by *Hypsilophodon foxii* it is reasonable to refer all the Morrison material to *Camptosaurus dispar*" (Galton & Powell, 1980 p. 2). Comparing trends in the growth of scapular blades of *Dysalotosaurus lettowvorbecki* with others iguanodontians, Hübner (2018) noted how the 'distal flaring' becomes more pronounced, but, as is evident from fig. 33, in the taxa examined the dorsal margin of the scapula segregates different species.

The humerus of SHN.JJS.015 is overall similar to that of *Uteodon aphanoecetes*, *Planicoxa venenica* and *Ouranosaurus nigeriensis* (Bertozzo et al., 2017; Carpenter & Wilson, 2008; DiCroce & Carpenter, 2001), being gracile in the proportions and development of its processes. This is in stark contrast with *Camptosaurus dispar*, which has a very stout humerus, associated with a robust pectoral girdle (Carpenter & Galton, 2018; Gilmore, 1909). In *Uteodon aphanoecetes* and *Planicoxa venenica*, the deltopectoral crest is rounded in profile (Carpenter & Wilson, 2008; DiCroce & Carpenter, 2001), being more prominent than in SHN.JJS.015 but less prominent than in *Camptosaurus dispar*. As mentioned above, the humeri of *Cumnoria prestwichii* are not well preserved, but Maidment et al. (2022, p. 3) indicated that "the deltopectoral crest of the humerus bears an oval muscle scar on its anterior surface" as an autapomorphy of *Cumnoria prestwichii*. This character is absent on the humeral shaft of SHN.JJS.015. Furthermore, the humerus of SHN.JJS.015 has a strongly arched profile in anteroposterior view, unlike the holotype of *Uteodon aphanoecetes* and the specimen USNM 5437 referred to *Camptosaurus dispar*. The same condition as the former is seen in specimen USNM 4248, referred to *Camptosaurus dispar* (holotype of *Camptosaurus browni*) (Fig. 6). The degree of variation in these specimens is assumed to be due to intraspecific variability (Carpenter & Lamanna, 2015; Carpenter & Wilson, 2008), although again no rigorous quantitative study of such variability has been conducted. It is clearly necessary to reappraise historical specimens in the light of new discoveries. Therefore, the attribution of SHN.JJS.015 to any taxon known from the Morrison

Formation seems unlikely, and we recognize the presence of a mosaic of features that, in combination, are unique to this specimen. However, given the paucity of a specimen represented so far by just five bones, and the absence of confidently asserted autapomorphic traits, we prefer not to erect a new taxon, even while recognizing that this specimen is unlikely to represent any other previously known ankylopollexian species. Thus, it is here considered to be an indeterminate member of Ankylopollexia.

The smaller specimens ML 434, SHN.JJS.073, and ML 2055 exhibit a general morphology that is consistent with immature ankylopollexians, including the following: the base of the fourth trochanter located at the midshaft of the femur, the insertion scar for the *Musculus caudofemoralis longus* not separated from the fourth trochanter, a U-shaped deep extensor groove in the distal epiphysis of the femoral shaft. These characters are shared with SHN.JJS.015, but given the scarcity of overlapping material, the lack of autapomorphic characters, and the recent increase in the diversity of iguanodontians in the Upper Jurassic of Portugal (Rotatori et al., 2023), it is not at present possible to determine whether these specimens all represent the same taxon. However, we note how the presence of a crest on the anterior surface of the shaft is shared among SHN.JJS.015, SHN.JJS.073, ML 434 and ML 2055, differentiating them from the *Draconyx loureiroi* holotype (Rotatori et al., 2022) and making referral to a single taxon the most likely scenario for the time being. In any event, despite the difficulties of taxonomic attribution, the discovery of such a disparity in size and mass reinforces the idea that the presence of large and thriving ankylopollexian populations in the ecosystems of the Lusitanian Basin was not an anomaly during the Late Jurassic (Fig. 12). This interpretation is corroborated by the rich and diverse ichnological record of iguanodontians in the Upper Jurassic of the Lusitanian Basin (Castanera et al., 2020).

Comparisons with other Late Jurassic Iberian ankylopollexians

Of the Late Jurassic European ankylopollexians, *Draconyx loureiroi* and *Oblitosaurus bunnueli* are the only species reported from the Iberian Peninsula to date (Mateus & Antunes, 2001; Rotatori et al., 2022; Sánchez-Fenollosa et al., 2023). However, remains from distinct ankylopollexian specimens have been reported

Figure 12. Reconstruction of a large-sized ankylopollexian iguanodontian dinosaur interacting with a juvenile in the Late Jurassic of Europe. Credit: Victor Carvalho, used with permission under CC BY-NC 4.0 licence.

from several Portuguese and Spanish localities (Galton, 1980; Ortega et al., 2009; Rotatori et al., 2020; Ruiz-Omeñaca et al., 2008), including the recently described specimen from the locality of Fuentecillas assigned to aff. *Camptosaurus* sp. by Sánchez-Fenollosa et al. (2022). One of these remains, an isolated right femur (MG 8801) from Torres Vedras, was initially referred to *Camptosaurus* sp. (Galton, 1980), but subsequently this bone was referred to *Draconyx loureiroi* (Mateus & Antunes, 2001) and interpreted as an indeterminate ankylopollexian iguanodontian by Escaso (2014). Only this specimen (MG 8801), together with the material from *Draconyx loureiroi* ML 357 (holotype specimen) and ML 434, and specimens ML 2042, ML 452, ML 864, MPA D-0087, MPA 664 and MPA D-0089 can be compared with SHN.JJS.015 (Rotatori et al., 2020, 2022; Sánchez-Fenollosa et al., 2022). Ankylopollexian material from the Andrés fossil site is scarce and consists only of tooth remains, and no comparisons can be made with SHN.JJS.015 (Malafaia et al., 2010).

The overall morphology of the SHN.JJS.015 dorsal vertebra is similar to that of specimens ML 452 and ML 864 (Rotatori et al., 2020, fig. 8). However, some differences associated with a presumably different position along the dorsal series can be observed. These are related to the orientation of the neural spine and transverse processes and the position of the parapophyses with respect to the transverse processes. In SHN.JJS.015 the neural spine is slightly posteriorly inclined, whereas in specimens ML 452 and ML 864 it is straight (Rotatori et al., 2020, fig. 8). Despite being incomplete, the morphology of the neural spine of the SHN.JJS.015 dorsal vertebra seems to be rectangular, as in specimens ML 452 and ML 864 (Rotatori et al., 2020, fig. 8). In SHN.JJS.015 the parapophyses are located on the ventral side of the transverse processes, so in dorsal view it is not possible to see them, unlike those of specimens ML 452 and ML 864, which are positioned anteriorly to their respective transverse processes (Rotatori et al., 2020, fig. 8). Like those of ML 864, the parapophyses in SHN.JJS.015 are positioned in a stepped facet with respect to the transverse processes. In the ML 452 dorsal vertebrae, the parapophyses are located in the same plane (Rotatori et al., 2020). In SHN.JJS.015 the transverse processes are upwardly oriented, as in the ML 864 but not the ML 452 dorsal vertebrae, even though these are judged to be positioned between the 10th and the 16th dorsal vertebral position, like SHN.JJS.015 (Rotatori et al., 2020). As far as MPA D-0087 is concerned, this element is an anterior dorsal centrum from Fuentecillas (Sánchez-Fenollosa et al., 2022, fig. 3f–j) and therefore cannot be directly compared to the vertebra of SHN.JJS.015.

Although the distalmost part of ML 2042 (Rotatori et al., 2020, fig. 8B) is not preserved, the scapula of SHN.JJS.015 can be distinguished from this latter specimen by its distal expansion towards the middle of the blade. In addition, the scapula of SHN.JJS.015 differs from ML 2042 in having a prominent and well-developed acromion process and glenoid and a cup-like supraglenoid fossa.

The distal region of the humerus in SHN.JJS.015 can be differentiated from that of the left humerus of the Fuentecillas specimen (MPA 664, MPA D-0089) in having ulnar and radial condyles of similar size and by the presence of wide V-shaped and shallow anterior and posterior intercondylar grooves (Sánchez-Fenollosa et al., 2022, fig. 6). In the Fuentecillas specimen, the ulnar condyle is larger than the radial condyle, and the posterior intercondylar groove is deeper and narrower than the anterior intercondylar groove (Sánchez-Fenollosa et al., 2022, fig. 6). Additionally, the radial condyle of SHN.JJS.015 does not present the arrow-shaped morphology observed in the Fuentecillas specimen (Sánchez-Fenollosa et al., 2022, fig. 6D).

The holotype specimen of *Draconyx loureiroi* (ML 357) preserves a right calcaneum attached to the tibia and fibula (Mateus & Antunes, 2001, fig. 9B–D; Rotatori et al., 2022, fig. 8B–F). The overall form of this bone is similar to that of other ankylopollexians. The femur of the holotype of *Draconyx loureiroi* (ML 357) can be distinguished from those of other ankylopollexians by a combination of femoral characters: (i) lacking a sharp crest extending from its medial condyle towards the lesser trochanter; (ii) a fully open U-shaped extensor groove; and (iii) the absence of a lateral projection into the fully open V-shaped flexor groove on the medial condyle (Rotatori et al., 2022).

These features cannot be observed in ML 434, a nearly complete left femur from Praia do Caniçal that lacks its distal part, which is assigned to *Draconyx loureiroi* (Mateus & Antunes, 2001) but considered to be an indeterminate ankylopollexian ornithopod by Escaso (2014) and recently by Rotatori et al. (2022). Overall, this femur is similar to those of '*Camptosaurus*' species, MG 8801 and SHN.JJS.015. As in these two femora and the Morrison Formation specimens that preserve the femur, ML 434 is curved and presents a crest that extends from the medial femoral condyle towards the lesser trochanter (Rotatori et al., 2022).

The femur of SHN.JJS.015 clearly differs from that of the holotype of *Draconyx loureiroi* (ML 357) by the presence of a strongly developed lateral projection into the flexor groove on the medial femoral condyle, forming a deep and fully open inverted J-shaped flexor groove; an enlarged posterior process of the medial condyle compared to its anterior process; a more laterally expanded anterior process of the medial condyle; a different outline of the medial margin of the medial condyle; and the development of a crest extending from its medial condyle towards the lesser trochanter (Rotatori et al., 2022).

SHN.JJS.015 can be distinguished from MG 8801 by some features observed in the distal femoral condyles (Escaso, 2014, fig. 6.3). However, some of the differences should be viewed with caution because the distal-most part of the surface of the MG 8801 femur is strongly abraded. Both the extensor and the flexor grooves in SHN.JJS.015 are deeper and narrower than those in MG 8801 (Escaso, 2014, fig. 6.3). The external margin of the medial condyle in MG 8801 is concave when viewed ventrally, whereas in SHN.JJS.015 the margin is convex (rounded). Another difference is the absence of a lateral projection into the flexor groove in the medial femoral condyle in MG 8801, but this may be explained by the strong abrasion of the preserved condyle surface (Escaso, 2014). Compared with what is observed in SHN.JJS.015, the inflection point of the curvature of the medial condyle is more anteriorly located in MG 8801 (Escaso, 2014, fig. 6.3). Like SHN.JJS.015, the femoral lesser trochanter is anteroposteriorly expanded, the posterior process of the medial condyle is enlarged with respect to the anterior process, and the anterior process of the lateral condyle is clearly laterally expanded in MG 8801 (Escaso, 2014). In MG 8801, the posterior process of the lateral condyle is not completely preserved, but it corresponds to a finger-like process that is less posteriorly elongated than in SHN.JJS.015. However, it is not possible to determine all its dimensions due to the abrasion mentioned above (Escaso, 2014).

As regards the recently described ankylopollexian *Oblitosaurus bunnueli* (Sánchez-Fenollosa et al., 2023), only the femora and calcanei can be compared. As in *Draconyx loureiroi*, the overall morphology of the calcaneum of *Oblitosaurus bunnueli* is similar to those of other ankylopollexians, including SHN.JJS.015. The femora of *Oblitosaurus bunnueli* and SHN.JJS.015 can be clearly differentiated. SHN.JJS.015 is distinguished from *Oblitosaurus bunnueli* by the absence of the autapomorphic femur characterized by a wide and robust lesser trochanter almost covering the lateral surface of the greater trochanter and by the absence of "[a medial condyle with] a pronounced and narrow lateromedial ridge on its ventral surface" (Sanchez-Fenollosa et al., 2023, p. 5). Furthermore, the femur of SHN.JJS.015 differs from *Oblitosaurus bunnueli* in having a strongly developed lateral projection into the flexor groove on the medial femoral condyle and an enlarged posterior process of the medial condyle compared to its anterior process.

The recently named *Hesperonyx martinhotomasorum* (Rotatori et al., 2023), an enigmatic dryomorphan of uncertain affinities, does not present any material that overlaps with the specimens discussed here, hampering the possibility of thorough comparisons. However, as recovered and discussed in the analysis of Rotatori et al. (2023), *H. martinhotomasorum* shows different affinities from SHN.JJS.015 and cannot be assigned to Ankylopollexia. As mentioned in the previous sections, the specimens discussed herein can be confidently assigned to this clade.

Ontogenetic trends in the ankylopollexian femora

Even though the isolated femora (ML 434, SHN.JJS.073, ML 2055) cannot be referred unambiguously to the same taxon as SHN.JJS.015, we can make some observations on the ontogenetic trends in the group. The differences in size are interpreted here as related to different ontogenetic stages, as has been suggested for other ornithopod populations in the Jurassic (Hübner, 2018). The overall proportions of the shaft are preserved during growth, whereas the fourth trochanter and the extensor groove become progressively more prominent. We also note that the smaller specimens (ML 2055 and SHN.JJS.073) possess a less pendant fourth trochanter than ML 434 and SHN.JJS.015. In addition, SHN.JJS.015 presents a small overhang over the flexor groove, which the smaller specimens lack. Not surprisingly, the acquisition of the mature traits is correlated with an increase in size, from the most immature stage (ML 2055, SHN.JJS.073) of approximately 100 kg to the weight of the fully grown individual of more than a ton (SHN.JJS.015). This trend has also been described in other iguanodontians (Hübner, 2018; Prieto-Marquéz, 2011; Verdú et al., 2015). Such transformations are known in populations of *Dysalotosaurus lettowvorbecki* (Hübner, 2018) and are associated with a progressive increase in size. Given the lack of material, we are unable to determine whether the species represented here was (or were) semiquadrupedal or bipedal like *Dysalotosaurus*. However, we hypothesize that the presence of the same trends associated with increasing size in different groups of iguanodontians indicates similar modular growth in Iguanodontia.

Palaeoecological and palaeobiogeographical implications

The evidence presented herein supports the presence of at least one large-sized ankylopollexian iguanodontian in the upper Kimmeridgian–lowermost Tithonian of the Lusitanian Basin (Fig. 12). Together with *Eousdryosaurus nanohallucis* (Escaso et al., 2014), *Draconyx loureiroi* (Mateus & Antunes, 2001), and *Hesperonyx martinhotomasorum* (Rotatori et al., 2023), the number of coeval iguanodontians thus rises to four forms. There are currently no grounds for synonymizing any of these taxa, although more complete specimens may lead to future taxonomic revisions. The presence of coeval, closely related ornithopod taxa was common in Early Cretaceous ecosystems, such as those recorded in the Wealden Group of the UK (Lockwood et al., 2021, 2024), the Bernissart mine in Belgium (Norman, 1980, 1986, 2004) and the Maestrazgo Basin of eastern Spain (Gasca et al., 2015; Gasulla et al., 2015, 2022; Medrano-Aguado et al., 2022; Verdú et al., 2018), as well as in the Late Cretaceous ecosystems of North America, Europe and Asia (Horner et al., 2004). However, it has not previously been reported in the Late Jurassic ecosystems of Europe. If the taxonomic interpretations suggested in this study stand, this indicates a very complex system of niche-partitioning among medium- to large-sized herbivores in the Late Jurassic of Portugal, exploiting different resources, as seen in other ecosystems (Mallon et al., 2012). Ornithopods attained high diversity within a low-disparity *bauplan*, and this defining condition of the clade was present as early as the Late Jurassic. This is also the first time that material from juvenile ankylopollexians that are likely to have shared the same landscape as adults has been formally described in the Lusitanian Basin (Fig. 12).

In palaeobiogeographical terms, the ornithopod described here increases the number of Late Jurassic early-branching iguanodontian taxa in Europe, confirming the old continent as a pivotal diversification point, as had already been predicted (Castanera et al., 2020; Rotatori et al., 2020, 2022). Rotatori et al. (2020) remarked on the importance of the Portuguese (and more generally Iberian) record of ornithopods in elucidating biogeographical patterns during the Late Jurassic. Traditionally, the Iberian Peninsula has always been associated with the Tendaguru Formation and the Morrison Formation in its palaeobiogeographical affinities (Galton, 1980; Mateus, 2006). Lately, several discoveries have highlighted the taxonomic peculiarities and distinctiveness of Iberian assemblages (Castanera et al., 2020; Escaso et al., 2014; Malafaia et al., 2020; Mateus et al., 2014; Mocho et al., 2014; Rotatori et al., 2022), while nonetheless confirming the generally close association with the abovementioned formations. The identification of this new large-sized ankylopollexian supports this tendency in that it is closely related to Morrison Formation taxa but not referable to the same species. The high diversity and distinctiveness of Iberian faunas casts doubt on the referral of some Iberian specimens to taxa recognized solely in the Morrison Formation (Sánchez-Fenollosa et al., 2022).

Conclusions

Here we describe and reassess iguanodontian material from the Upper Jurassic of Portugal, recovered in the Lusitanian Basin. The largest specimen, SHN.JJS.015, is a remarkable, large-sized, indeterminate ankylopollexian possessing a mosaic of characters in the humerus, scapula and femur that prevent attribution to any known taxa. Phylogenetically, SHN.JJS.015 is recovered as an ankylopollexian, in a polytomy with *Camptosaurus dispar* and Styracosterna. In addition, we describe three other fragmentary specimens (ML 434, SHN.JJS.073, ML 2055) of indeterminate ankylopollexian affinities, which suggest that this clade was relatively common in the ecosystem of the Late Jurassic Lusitanian Basin. The description of SHN.JJS.015 adds a new member of Ankylopollexia to the poorly known Late Jurassic iguanodontian fauna of the Iberian landmasses and confirms the coexistence, at least during the lowermost part of the Tithonian, of three medium- to large-sized ankylopollexian ornithopods in south-western Europe, highlighting a complex system of ecological niche-partitioning involving *Draconyx loureiroi*, *Oblitosaurus bunnueli* and SHN.JJS.015. Furthermore, it supports the interpretation of Europe as a pivotal region of diversification for early-diverging iguanodontians during the Late Jurassic and shows the fundamental role of Iberian landmasses in achieving a better understanding of biogeographical patterns.

Acknowledgements

We thank the technical staff of the Museu da Lourinhã and the Sociedade de História Natural de Torres Vedras for their support during these years of study. Rupert Glasgow revised the English grammar. This work was supported by the National Funds through the FCT – Fundação para a Ciencia e a Tecnología, I.P. through Research Unit UIDB/04035/2020 (https://doi.org/10.54499/UIDB/04035/2020), Project PTDC/CTA-PAL/2217/2021, the programmes CEECIND/01770/2018 (EM) and CEECIND/00726/2017 (PM), and the grant SFRH/BD/146230/2019 (FMR) and COVID/BD/153554/2024 (FMR). MMA is supported by the MCIN/AEI/10.13039/501100011033 and cofinanced by the NextGeneration EU/PRTR, Ramón y Cajal contract

RYC2021-034473-I and the Ministerio de Ciencia e Innnovación with the grant PID2021-122612OB-100. This research was also funded by a Jurassic Foundation grant to FMR.

We are grateful for the contribution of two anonymous reviewers that greatly improved the quality of the manuscript. We also thank Dr Victoria Arbour, editor of the journal, for additional comments and stylistic suggestions that greatly improved the final version of the manuscript.

Funding

This work was supported by the National Funds through the FCT - Fundação para a Ciencia e a Tecnología, NextGeneration EU, Ministerio de Ciencia e Innovación, Jurassic Foundation. para a Ciencia e a Tecnologıa, I.P. through Research Unit UIDB/04035/2020 (https://doi.org/10.54499/UIDB/04035/2020), Project PTDC/CTA-PAL/2217/2021, the programmes CEECIND/01770/2018 (EM) and CEECIND/00726/2017 (PM), and the grant SFRH/BD/146230/2019 (FMR) and COVID/BD/153554/2024 (FMR). MMA is supported by the MCIN/AEI/10.13039/501100011033 and cofinanced by the NextGeneration EU/PRTR, Ramon y Cajal contract RYC2021-034473-I and the Ministerio de Ciencia e Innnovacion with the grant PID2021-122612OB-100. This research was also funded by a Jurassic Foundation grant to FMR.

Disclosure statement

No potential conflict of interest was reported by the author(s).

Supplemental material

Supplemental material for this article can be accessed here: https://doi.org/10.1080/14772019.2025.2470789.

ORCID

Filippo Maria Rotatori http://orcid.org/0000-0002-7084-1919
Fernando Escaso http://orcid.org/0000-0001-7642-1555
Bruno Camilo http://orcid.org/0000-0003-3202-5010
Filippo Bertozzo http://orcid.org/0000-0002-0917-9989
Elisabete Malafaia http://orcid.org/0000-0003-4894-4257
Octávio Mateus http://orcid.org/0000-0003-1253-3616
Pedro Mocho http://orcid.org/0000-0002-3348-5572
Francisco Ortega http://orcid.org/0000-0002-7431-354X
Miguel Moreno-Azanza http://orcid.org/0000-0002-7210-1033

References

Antunes, M. T., & **Mateus, O.** (2003). Dinosaurs of Portugal. *Comptes Rendus Palevol*, *2*, 77–95. https://doi.org/10.1016/S1631-0683(03)00003-4

Barrett, P. M., **Butler, R. J.**, **Twitchett, R. J.**, & **Hutt, S.** (2011). New material of *Valdosaurus canaliculatus* (Ornithischia: Ornithopoda) from the Lower Cretaceous of southern England. *Special Papers in Palaeontology*, *86*, 131–163.

Benson, R. B., **Hunt, G.**, **Carrano, M. T.**, & **Campione, N.** (2018). Cope's rule and the adaptive landscape of dinosaur body size evolution. *Palaeontology*, *61*(1), 13–48. https://doi.org/10.1111/pala.12329

Bertozzo, F., **Dalla Vecchia, F. M.**, & **Fabbri, M.** (2017). The Venice specimen of *Ouranosaurus nigeriensis* (Dinosauria, Ornithopoda). *PeerJ*, *5*, e3403. https://doi.org/10.7717/peerj.3403

Bertozzo, F., **Silva, B.**, **Martill, D.**, **Vorderwülbecke, E.**, **Aureliano, T.**, **Schouten, R.**, & **Aquino, P.** (2021). A large pterosaur femur from the Upper Jurassic (Lusitanian Basin) of Portugal. *Acta Palaeontologica Polonica*, *66*. https://doi.org/10.4202/app.00858.2020

Carpenter, K., & **Galton, P. M.** (2018). A photo documentation of bipedal ornithischian dinosaurs from the Upper Jurassic Morrison Formation, USA. *Geology of the Intermountain West*, *5*, 167–207. https://doi.org/10.31711/giw.v5.pp167-207

Carpenter, K., & **Lamanna, M. C.** (2015). The braincase assigned to the ornithopod dinosaur *Uteodon* McDonald, 2011, reassigned to *Dryosaurus* Marsh, 1894: Implications for iguanodontian morphology and taxonomy. *Annals of Carnegie Museum*, *83*(2), 149–165. https://doi.org/10.2992/007.083.0201

Carpenter, K., & **Wilson, Y.** (2008). A new species of *Camptosaurus* (Ornithopoda: Dinosauria) from the Morrison Formation (Upper Jurassic) of Dinosaur National Monument, Utah, and a biomechanical analysis of its forelimb. *Annals of Carnegie Museum*, *76*, 227–264. https://doi.org/10.2992/0097-4463(2008)76[227:ANSOCO]2.0.CO;2

Castanera, D., **Silva, B. C.**, **Santos, V. F.**, **Malafaia, E.**, & **Belvedere, M.** (2020). Tracking Late Jurassic ornithopods in the Lusitanian Basin of Portugal: Ichnotaxonomic implications. *Acta Palaeontologica Polonica*, *65*, 399–412. https://doi.org/10.4202/app.00707.2019

Chiarenza, A. A., **Fabbri, M.**, **Consorti, L.**, **Muscioni, M.**, **Evans, D. C.**, **Cantalapiedra, J. L.**, & **Fanti, F.** (2021). An Italian dinosaur Lagerstätte reveals the tempo and mode of hadrosauriform body size evolution. *Scientific*

Reports, *11*(1), 23295. https://doi.org/10.1038/s41598-021-02490-x

Costa, F., & **Mateus, O.** (2019). Dacentrurine stegosaurs (Dinosauria): A new specimen of *Miragaia longicollum* from the Late Jurassic of Portugal resolves taxonomical validity and shows the occurrence of the clade in North America. PLoS ONE, *14*(11), e0224263. https://doi.org/10.1371/journal.pone.0224263

DiCroce, T., & **Carpenter, K.** (2001). New ornithopod from the Cedar Mountain Formation (Lower Cretaceous) of eastern Utah. In D. H. Tanke & K. Carpenter (Eds.), *Mesozoic vertebrate life* (pp. 183–196). Indiana University Press.

Dieudonné, P.-E., **Cruzado-Caballero, P.**, **Godefroit, P.**, & **Tortosa, T.** (2020). A new phylogeny of cerapodan dinosaurs. *Historical Biology*, *0*, 1–21. https://doi.org/10.1080/08912963.2020.1793979

Dollo, L. (1888). Iguanodontidae et Camptonotidae. *Comptes Rendus de l'Académie des Sciences de Paris*, *106*, 775–777.

Escaso, F. (2014). *Historia Evolutiva de Los Ornithischia (Dinosauria) Del Jurásico Superior de Portugal*. Universidad Autónoma de Madrid.

Escaso, F., **Ortega, F.**, **Dantas, P.**, **Malafaia, E.**, **Pimentel N. L.**, **Pereda-Suberbiola, X.**, **Sanz, J. L.**, **Kullberg, J. C.**, **Kullberg, M. C.**, & **Barriga, F.** (2007). New evidence of shared dinosaur across Upper Jurassic Proto-North Atlantic: *Stegosaurus* from Portugal. *Naturwissenschaften*, *94*, 367–374. https://doi.org/10.1007/s00114-006-0209-8

Escaso, F., **Ortega, F.**, **Dantas, P.**, **Malafaia, E.**, **Silva, B.**, **Gasulla, J. M.**, **Mocho, P.**, **Narváez, I.**, & **Sanz, J. L.** (2014). A new dryosaurid ornithopod (Dinosauria, Ornithischia) from the Late Jurassic of Portugal. *Journal of Vertebrate Paleontology*, *34*, 1102–1112. https://doi.org/10.1080/02724634.2014.849715

Foster, J. (2020). *Jurassic West, Second Edition: The dinosaurs of the Morrison formation and their world* (NED-New edition, p. 2). Indiana University Press. https://doi.org/10.2307/j.ctv18sqxpx

Fürsich, F. T. (1981). Salinity-controlled benthic associations from the Upper Jurassic of Portugal. *Lethaia*, *14*, 203–223. https://doi.org/10.1111/j.1502-3931.1981.tb01690.x

Fürsich, F. T., **Schneider, S.**, **Werner, W.**, **Lopez-Mir, B.**, & **Pierce, C. S.** (2022). Life at the continental–marine interface: Palaeoenvironments and biota of the Alcobaça Formation (Late Jurassic, Central Portugal), with a formal definition of the unit appended. *Palaeobiodiversity and Palaeoenvironments*, *102*, 265–329. https://doi.org/10.1007/s12549-021-00496-x

Galton, P. M. (1980). European Jurassic ornithopod dinosaurs of the families Hypsilophodontidae and Camptosauridae. *Neues Jahrbuch für Geologie und Paläontologie, Abhandlungen*, *160*, 73–95. https://doi.org/10.1127/njgpa/160/1980/73

Galton, P. M. (1981). *Dryosaurus*, a hypsilophodontid dinosaur from the Upper Jurassic of North America and Africa postcranial skeleton. *Paläontologische Zeitschrift*, *55*, 271–312. https://doi.org/10.1007/BF02988144

Galton, P. M., & **Powell, H. P.** (1980). The ornithischian dinosaur *Camptosaurus prestwichii* from the Upper Jurassic of England. *Palaeontology*, *23*, 411–443.

Gasca, J. M., **Canudo, J. I.**, **Ruiz-Omeñaca, J. I.**, & **Moreno-Azanza, M.** (2015). New material and phylogenetic position of the basal iguanodont dinosaur *Delapparentia turolensis* from the Barremian (Early Cretaceous) of Spain. *Journal of Iberian Geology*, *41*(1), 57–70. https://doi.org/10.5209/rev_JIGE.2015.v41.n1.48655

Gasulla, J. M., **Escaso, F.**, **Narváez, I.**, **Ortega, F.**, & **Sanz, J. L.** (2015). A new sail-backed styracosternan (Dinosauria: Ornithopoda) from the Early Cretaceous of Morella, Spain. *PLoS One*, *10*, e0144167. https://doi.org/10.1371/journal.pone.0144167

Gasulla, J. M., **Escaso, F.**, **Narváez, I.**, **Sanz, J. L.**, & **Ortega, F.** (2022). New *Iguanodon bernissartensis* axial bones (Dinosauria, Ornithopoda) from the Early Cretaceous of Morella, Spain. *Diversity*, *14*, 63. https://doi.org/10.3390/d14020063

Gilmore, C. W. (1909). Osteology of the Jurassic reptile *Camptosaurus*, with a revision of the species of the genus, and description of two new species. *Proceedings of the United States National Museum*, *36*, 197–332. https://doi.org/10.5479/si.00963801.36-1666.197

Gilmore, C. W. (1925). Osteology of ornithopodous dinosaurs from Dinosaur National Monument, Utah. Part I. On a skeleton of *Camptosaurus medius* Marsh. Part II. On a skeleton of Dryosaurus altus Marsh. Part III. On a skeleton of Laosauruls gracilis Marsh. *Memoirs of the Carnegie Museum*, *10*, 385–410.

Goloboff, P. A., & **Catalano, S. A.** (2016). TNT version 1.5, including a full implementation of phylogenetic morphometrics. *Cladistics*, *32*, 221–238. https://doi.org/10.1111/cla.12160

Guillaume, A. R. D., **Moreno-Azanza, M.**, **Puértolas-Pascual, E.**, & **Mateus, O.** (2020). Palaeobiodiversity of crocodylomorphs from the Lourinhã Formation based on the tooth record: Insights into the palaeoecology of the Late Jurassic of Portugal. *Zoological Journal of the Linnean Society*, *189*, 549–583. https://doi.org/10.1093/zoolinnean/zlz112

Guillaume, A. R. D., **Natário, C.**, **Mateus, O.**, & **Moreno-Azanza, M.** (2022). Plasticity in the morphology of the fused frontals of Albanerpetontidae (Lissamphibia; Allocaudata). *Historical Biology*, *35*(4), 537–554. https://doi.org/10.1080/08912963.2022.2054712

Griffin, C. T., **Stocker, M. R.**, **Colleary, C.**, **Stefanic, C. M.**, **Lessner, E. J.**, **Riegler, M.**, **Formoso, K.**, **Koeller, K.**, & **Nesbitt, S. J.** (2021). Assessing ontogenetic maturity in extinct saurian reptiles. *Biological Reviews*, *96*(2), 470–525. https://doi.org/10.1111/brv.12666

Hill, G. (1988). *The sedimentology and lithostratigraphy of the Upper Jurassic Lourinhã Formation, Lusitanian Basin, Portugal*. [Unpublished PhD thesis]. Open University, Milton Keynes, UK.

Horner, J. R., **De Ricqlès, A.**, **Padian, K.**, & **Scheetz, R. D.** (2009). Comparative long bone histology and growth of the 'hypsilophodontid' dinosaurs *Orodromeus makelai*, *Dryosaurus altus*, and *Tenontosaurus tillettii* (Ornithischia: Euornithopoda). *Journal of Vertebrate Paleontology*, *29*, 734–747. https://doi.org/10.1671/039.029.0312

Horner, J. R., **Weishampel, D. B.**, & **Forster, C.** (2004). Hadrosauridae. In: Weishampel, D. B., Dodson, P., & Osmolska, H. (Eds.), *The Dinosauria: Second Edition* (pp. 438–463). University of California Press.

Hübner, T. (2012). Bone histology in Dysalotosaurus lettowvorbecki (Ornithischia: Iguanodontia) –variation, growth, and implications. *PLoS ONE*, *7*(1), e29958.

Hübner, T. (2018). The postcranial ontogeny of *Dysalotosaurus lettowvorbecki* (Ornithischia: Iguanodontia) and implications for the evolution of ornithopod dinosaurs. *Palaeontographica Abteilung A*, 43–120. https://doi.org/10.1127/pala/2018/0072

Kilbourne, B. M., & **Makovicky, P. J.** (2010). Limb bone allometry during postnatal ontogeny in non-avian dinosaurs. *Journal of Anatomy*, *217*(2), 135–152.

Kullberg, J. C., **Rocha, R. B.**, **Soares, A. F.**, **Rey, J.**, **Terrinha, P.**, **Azerêdo, A. C.**, **Callapez, P.**, **Duarte, L. V.**, **Kullberg, M. C.**, **Martins, L.**, **Miranda, J. R.**, **Alves, C.**, **Mata, J.**, **Madeira, J.**, **Mateus, O.**, **Moreira, M.**, & **Nogueira, C. R.** (2013). A Bacia Lusitaniana: Estratigrafia, Paleogeografia e Tectónica. In R. Dias, A. Araújo, P. Terrinha, & J. C. Kullberg (Eds.), Geologia de Portugal no contexto da Ibéria (pp. 989–1141). Escolar Editora.

Lapparent, A. F., & **Zbyszewski, G.** (1957). Les dinosauriens du Portugal. *Memórias dos Serviços Geológicos de Portugal*, *2*, 1–63.

Leinfelder, R. R. (1986). Facies, stratigraphy and paleogeographic analysis of Upper? Kimmeridgian to Upper Portlandian sediments in the environs of Arruda dos Vinhos, Estremadura, Portugal. *Münchner Geowiss, Abhandlungen*, *7*, 1–215.

Lockwood, J. A., **Martill, D. M.**, & **Maidment, S. C.** (2021). A new hadrosauriform dinosaur from the Wessex Formation, Wealden Group (Early Cretaceous), of the Isle of Wight, southern England. *Journal of Systematic Palaeontology*, *19*, 847–888. https://doi.org/10.1080/14772019.2021.1978005

Lockwood, J. A. F., **Martill, D. M.**, & **Maidment, S. C. R.** (2024). Comptonatus chasei, a new iguanodontian dinosaur from the Lower Cretaceous Wessex Formation of the Isle of Wight, southern England. *Journal of Systematic Palaeontology*, *22*(1). https://doi.org/10.1080/14772019.2024.2346573

López-Rojas, V., **Mateus, S.**, **Marinheiro, J.**, **Mateus, O.**, & **Puértolas-Pascual, E.** (2024). A new goniopholidid crocodylomorph from the Late Jurassic of Portugal. *Palaeontologia Electronica*, *27*(1), 1–33. https://doi.org/10.26879/1316palaeo-electronica.org/content/2024/5106-a-new-portuguese-goniopholidid

Madzia, D., **Arbour, V. M.**, **Boyd, C. A.**, **Farke, A. A.**, **Cruzado-Caballero, P.**, & **Evans, D. C.** (2021). The phylogenetic nomenclature of ornithischian dinosaurs. *PeerJ*, *9*, e12362. https://doi.org/10.7717/peerj.12362

Maidment, S. C. R., **Chapelle, K. E. J.**, **Bonsor, J. A.**, **Button, D.**, & **Barrett, P.** (2022). Osteology and Relationship of *Cumnoria prestwichii* (Ornithischia: Ornithopoda) from the Late Jurassic of Oxfordshire, UK. *Monograph of the Palaeontographical Society*, *664*(175), 1–55. https://doi.org/10.1080/02693445.2022.2162669

Malafaia, E., **Mocho, P.**, **Escaso, F.**, & **Ortega, F.** (2020). A new carcharodontosaurian theropod from the Lusitanian Basin: Evidence of allosauroid sympatry in the European Late Jurassic. *Journal of Vertebrate Paleontology*, *40*, e1768106. https://doi.org/10.1080/02724634.2020.1768106

Malafaia, E., **Ortega, F.**, **Escaso, F.**, **Dantas, P.**, **Pimentel, N.**, **Gasulla, J. M.**, **Ribeiro, B.**, **Barriga, F.**, & **Sanz, J. L.** (2010). Vertebrate fauna at the *Allosaurus* fossil-site of Andrés (Upper Jurassic), Pombal, Portugal. *Journal of Iberian Geology*, *36*(2), 193–204. https://doi.org/10.5209/rev_JIGE.2010.v36.n2.7

Mallon, J. C., **Evans, D. C.**, **Ryan, M. J.**, & **Anderson, J. S.** (2012). Megaherbivorous dinosaur turnover in the Dinosaur Park Formation (upper Campanian) of Alberta, Canada. *Palaeogeography, Palaeoclimatology, Palaeoecology*, *350*, 124–138. https://doi.org/10.1016/j.palaeo.2012.06.024

Manuppella, G. (1998). Geologic data about the 'Camadas de Alcobaça' (Upper Jurassic) North of Lourinhã, and facies variation. Memórias da Academia de Ciências de Lisboa, *37*, 17–24.

Manuppella, G., **Antunes, M. T.**, **Pais, J.**, **Ramalho, M. M.**, & **Rey, J.** (1999). Notícia explicativa da Folha 30-A (Lourinhã). Departamento de Geologia do Instituto Geolégico e Minerio.

Marsh, O. C. (1881). Principal characters of American Jurassic dinosaurs, Part IV. *American Journal of Science* (Serie 3), *21*, 167–170. https://doi.org/10.2475/ajs.s3-21.122.167

Mateus, O. (1998). *Lourinhanosaurus antunesi*, a new upper Jurassic allosauroid (Dinosauria: Theropoda) from Lourinhã, Portugal. *Memórias da Academia de Ciências de Lisboa*, *37*, 111–124.

Mateus, O. (2006). Late Jurassic dinosaurs from the Morrison Formation (USA), the Lourinha and Alcobaça formations (Portugal), and the Tendaguru Beds (Tanzania): A comparison. *New Mexico Museum of Natural History and Science Bulletin*, *36*, 223–231.

Mateus, O., & **Antunes, M.** (2001). *Draconyx loureiroi*, a new Camptosauridae (Dinosauria, Ornithopoda) from the Late Jurassic of Lourinhã, Portugal. *Annales de Paléontologie*, *87*, 61–73. https://doi.org/10.1016/S0753-3969(01)88003-4

Mateus, O., **Dinis, J.**, & **Cunha, P. P.** (2017). The Lourinhã Formation: The Upper Jurassic to lower most Cretaceous of the Lusitanian Basin, Portugal – landscapes where dinosaurs walked. *Ciências da Terra – Earth Sciences Journal*, *19*, 75–97. https://doi.org/10.21695/cterra/esj.v19i1.355

Mateus, O., **Maidment, S. C.**, & **Christiansen, N. A.** (2009). A new long-necked 'sauropod-mimic' stegosaur and the evolution of the plated dinosaurs. *Proceedings of the Royal Society B: Biological Sciences*, *276*, 1815–1821. https://doi.org/10.1098/rspb.2008.1909

Mateus, O., **Mannion, P. D.**, & **Upchurch, P.** (2014). *Zby atlanticus*, a new turiasaurian sauropod (Dinosauria, Eusauropoda) from the Late Jurassic of Portugal. *Journal of Vertebrate Paleontology*, *34*, 618–634. https://doi.org/10.1080/02724634.2013.822875

McDonald, A. T. (2011). The taxonomy of species assigned to *Camptosaurus* (Dinosauria: Ornithopoda). *Zootaxa*, *2783*, 52–68. https://doi.org/10.11646/zootaxa.2783.1.4

McDonald, A. T. (2012). Phylogeny of Basal Iguanodonts (Dinosauria: Ornithischia): An update. *PloS One*, *7*(5), e36745. https://doi.org/10.1371/journal.pone.0036745

Medrano-Aguado, E., **Parrilla-Bel, J.**, **Gasca, J. M.**, **Alonso, A.**, & **Canudo, J. I.** (2022). Ornithopod diversity in the Lower Cretaceous of Spain: New styracosternan remains from the Barremian of the Maestrazgo Basin (Teruel province, Spain). *Cretaceous Research*, *144*, 105458. https://doi.org/10.1016/j.cretres.2022.105458

Mocho, P., **Royo-Torres, R.**, **Escaso, F.**, **Malafaia, E.**, **de Miguel Chaves, C.**, **Narváez, I.**, **Pérez-García, A.**, **Pimentel, N.**, **Silva, B. C.**, & **Ortega, F.** (2017). Upper Jurassic sauropod record in the Lusitanian Basin

(Portugal): Geographical and lithostratigraphical distribution. P*alaeontologia Electronica*, *20*.2.27A, 1–50, https://palaeo-electronica.org/content/2017/1856-portuguese-sauropods

Mocho, P., **Royo-Torres, R.**, **Malafaia, E.**, **Escaso, F.**, & **Ortega, F.** (2017). Sauropod tooth morphotypes from the Upper Jurassic of the Lusitanian Basin (Portugal). *Papers in Palaeontology*, *3*, 259–295. https://doi.org/10.1002/spp2.1075

Mocho, P., **Royo-Torres, R.**, **Malafaia, E.**, **Escaso, F.**, **Silva, B.**, & **Ortega, F.** (2016). Turiasauria-like teeth from the Upper Jurassic of the Lusitanian Basin, Portugal. *Historical Biology*, *28*, 861–880. https://doi.org/10.1080/08912963.2015.1049948

Mocho, P., **Royo-Torres, R.**, & **Ortega, F.** (2014). Phylogenetic reassessment of *Lourinhasaurus alenquerensis*, a basal Macronaria (Sauropoda) from the Upper Jurassic of Portugal. *Zoological Journal of the Linnean Society*, *170*, 875–916. https://doi.org/10.1111/zoj.12113

Mocho, P., **Royo-Torres, R.**, & **Ortega, F.** (2019). A new macronarian sauropod from the Upper Jurassic of Portugal. *Journal of Vertebrate Paleontology*, *39*, e1578782. https://doi.org/10.1080/02724634.2019.1578782

Norman, D. B. (1980). On the ornithischian dinosaur *Iguanodon bernissartensis* from the lower Lower Cretaceous of Bernissart (Belgium). Memoir de l'Institut Royal des Sciences *Naturelles de Belgique*, *178*, 1–105.

Norman, D. B. (1986). On the anatomy of *Iguanodon atherfieldensis* (Ornithischia: Ornithopoda). Bulletin de l'Institut royal des Sciences *naturelles de Belgique*, *56*, 281–372.

Norman, D. B. (1998). On Asian ornithopods (Dinosauria: Ornithischia). 3. A new species of iguanodontid dinosaur. *Zoological Journal of the Linnean Society*, *122*, 291–348. https://doi.org/10.1111/j.1096-3642.1998.tb02533.x

Norman, D. B. (2004). Basal Iguanodontia. In D. B. Weishampel, P. Dodson, & H. Osmolska (Eds.), *The Dinosauria: Second Edition* (pp. 413–437). University of California Press, Berkeley.

Norman, D. B. (2015). On the history, osteology, and systematic position of the Wealden (Hastings group) dinosaur *Hypselospinus fittoni* (Iguanodontia: Styracosterna). *Zoological Journal of the Linnean Society*, *173*, 92–189. https://doi.org/10.1111/zoj.12193

Ortega, F. (2009). Faunas de répteis do Jurássico Superior de Portugal. *Paleolusitana*, *1*, 43–56.

Owen, R. (1842). Report on British fossil reptiles, Part II. *Reports of the British Association for the Advancement of Science*, *11*, 60–204.

Pena dos Reis, R. P. B., **Proença Cunha, C. P.**, **Dinis, J. L.**, & **Trincão, P. R.** (2000). Geologic evolution of the Lusitanian Basin (Portugal) during the late Jurassic. *GeoResearch Forum*, *6*, 345–356.

Poole, K. (2022). Phylogeny of iguanodontian dinosaurs and the evolution of quadrupedality. *Palaeontologia Electronica*, *25*, 1–65. https://doi.org/10.26879/702

Poole, K. (2023). Placing juvenile specimens in phylogenies: An ontogenetically sensitive phylogenetic assessment of a new genus of iguanodontian dinosaur from the Early Cretaceous Kirkwood Formation, South Africa. *Anatomical Record*, *306*(7), 1939–1950. https://doi.org/10.1002/ar.25095

Prieto-Márquez, A. (2011). Cranial and appendicular ontogeny of Bactrosaurus johnsoni, a hadrosauroid dinosaur from the Late Cretaceous of northern China. Palaeontology, *54*(4), 773–792.

Prieto-Márquez, A., **Fondevilla, V.**, **Sellés, A. G.**, **Wagner, J. R.**, & **Galobart, À** (2019). *Adynomosaurus arcanus*, a new lambeosaurine dinosaur from the Late Cretaceous Ibero-Armorican Island of the European archipelago. *Cretaceous Research*, *96*, 19–37. https://doi.org/10.1016/j.cretres.2018.12.002

Rasmussen, E. S., **Lomholt, S.**, **Andersen, C.**, & **Vejbaek, O. V.** (1998). Aspects of the structural evolution of the Lusitanian Basin in Portugal and the shelf and slope area offshore Portugal. *Tectonophysics*, *300*, 199–225. https://doi.org/10.1016/S0040-1951(98)00241-8

Rey, J. (1999). Lower Cretaceous depositional sequences in the Cascais Area. In European Palaeontological Association Workshop: Field trip A. (pp. 1–57). Lisboa.

Rocha, R. B. (coord.), **Marques, B. L.**, **Kullberg, J. C.**, **Caetano, P. C.**, **Lopes, C.**, **Soares, A. F.**, **Duarte, L. V.**, **Marques, J. F.**, & **Gomes, C. R.** (1996). *The 1st and 2nd rifting phases of the Lusitanian Basin: Stratigraphy, sequence analysis and sedimentary evolution*. Final Report C. E. C. Proj. MILUPOBAS, Lisboa.

Rocha, R. B., & **Soares, A. F.** (1984). Algumas reflexões sobre a sedimentação jurássica na orla mesocenozóica ocidental de Portugal. *Memórias e Notícias*, *97*, 133–142.

Rotatori, F. M., **Ferrari, L.**, **Sequero, C.**, **Camilo, B.**, **Mateus, O.**, & **Moreno-Azanza, M.** (2023). An unexpected early-diverging iguanodontian dinosaur (Ornithischia, Ornithopoda) from the Upper Jurassic of Portugal. *Journal of Vertebrate Paleontology*, *43*(4). https://doi.org/10.1080/02724634.2024.2310066

Rotatori, F. M., **Moreno-Azanza, M.**, & **Mateus, O.** (2020). New information on ornithopod dinosaurs from the Late Jurassic of Portugal. *Acta Palaeontologica Polonica*, *65*, 35–57. https://doi.org/10.4202/app.00661.2019

Rotatori, F. M., **Moreno-Azanza, M.**, & **Mateus, O.** (2022). Reappraisal and new material of the holotype of *Draconyx loureiroi* (Ornithischia: Iguanodontia) provide insights on the tempo and mode of evolution of thumb-spiked dinosaurs. *Zoological Journal of the Linnean Society*, *zlab113*. https://doi.org/10.1093/zoolinnean/zlab113

Rotatori, F. M., **Quaranta, M.**, **Bertozzo, F.**, **Hübner, T.**, **Camilo, B.**, **Mateus, O.**, & **Moreno-Azanza, M.** (2024). Hadrosaur-like vascularisation in the dentary of an early diverging iguanodontian dinosaur. *Historical Biology*, *36*(10), 1979–1984. https://doi.org/10.1080/08912963.2023.2238727

Ruiz-Omeñaca, J. I., **Pereda Suberbiola, X.**, & **Galton, P. M.** (2006). Callovosaurus leedsi, the earliest dryosaurid dinosaur (Ornithischia: Euornithopoda) from the Middle Jurassic of England. In K. Carpenter (Ed.), *Horns and beaks: Ceratopsian and ornithopod dinosaurs* (p. 316). Indiana University Press.

Ruiz-Omeñaca, J. I., **Piñuela, L.**, & **García-Tamos, J. C.** (2008). Nuevos restos de ornitópodo (Ornithischia: Ankylopollexia) del Jurásico Superior de Tazones, Asturias (Formación Tereñes). *Geogaceta*, *45*, 59–62.

Sánchez-Fenollosa, S., **Verdú, F. J.**, & **Cobos, A.** (2023). The largest ornithopod (Dinosauria: Ornithischia) from the Upper Jurassic of Europe sheds light on the evolutionary history of basal ankylopollexians. *Zoological Journal of* *the Linnean Society*, *zlad076*, *199*(4), 1013–1033. https://doi.org/10.1093/zoolinnean/zlad076

Sánchez-Fenollosa, S., **Verdú, F. J.**, **Suñer, M.**, & **de Santisteban, C.** (2022). Tracing Late Jurassic ornithopod diversity in the eastern Iberian Peninsula: *Camptosaurus*-like postcranial remains from Alpuente (Valencia, Spain). *Journal of Iberian Geology*, *48*, 65–78. https://doi.org/10.1007/s41513-021-00182-z

Seeley, H. G. (1887). On the classification of the fossil animals commonly named Dinosauria. *Proceedings of the Royal Society of London*, *43*, 165–171.

Sereno, P. C. (1986). Phylogeny of the bird-hipped dinosaurs (Order Ornithischia). *National Geographic Research*, *2*(2), 234–256.

Takasaki, R., **Fiorillo, A. R.**, **Tykoski, R. S.**, & **Kobayashi, Y.** (2020). Re-examination of the cranial osteology of the Arctic Alaskan hadrosaurine with implications for its taxonomic status. *PLoS One*, *15*, e0232410. https://doi.org/10.1371/journal.pone.0232410

Taylor, A. M., **Gowland, S.**, **Leary, S.**, **Keogh, Kevin J.**, & **Martinius, A. W.** (2014). Stratigraphical correlation of the Late Jurassic Lourinhã Formation in the Consolação sub-basin (Lusitanian Basin), Portugal: Lourinhã Formation stratigraphy. *Geological Journal*, *49*, 143–162. https://doi.org/10.1002/gj.2505

Thulborn, R. A. (1973). Teeth of ornithischian dinosaurs from the Upper Jurassic of Portugal. Contribuiçao para o Conhecimento da Fauna do Kimeridgiano da Mina de Lignito Guimarota (Leiria, Portugal) III Parte, VI. *Memórias dos Serviços geológicos de Portugal,(nova Sér.)*, *22*, 89–134.

Verdú, F. J., **Godefroit, P.**, **Royo-Torres, R.**, **Cobos, A.**, & **Alcalá, L.** (2017). Individual variation in the postcranial skeleton of the Early Cretaceous *Iguanodon bernissartensis* (Dinosauria: Ornithopoda). *Cretaceous Research*, *74*, 65–86. https://doi.org/10.1016/j.cretres.2017.02.006

Verdú, F. J., **Royo-Torres, R.**, **Cobos, A.**, & **Alcala, L.** (2015). Perinates of a new species of Iguanodon (Ornithischia: Ornithopoda) from the lower Barremian of Galve (Teruel, Spain). *Cretaceous Research*, *56*, 250–264.

Verdú, F. J., **Royo-Torres, R.**, **Cobos, A.**, & **Alcalá, L.** (2018). New systematic and phylogenetic data about the early Barremian *Iguanodon galvensis* (Ornithopoda: Iguanodontoidea) from Spain. *Historical Biology*, *30*, 437–474. https://doi.org/10.1080/08912963.2017.1287179

Vidarte, C. F., **Calvo, M. M.**, **Fuentes, F. M.**, & **Fuentes, M. M.** (2016). Un nuevo dinosaurio estiracosterno (Ornithopoda: Ankylopollexia) del Cretácico Inferior de España. *Spanish Journal of Palaeontology*, *31*, 407–446.

Xu, X., **Tan, Q.**, **Gao, Y.**, **Bao, Z.**, **Yin, Z.**, **Guo, B.**, **Wang, J.**, **Tan, L.**, **Zhang, Y.**, & **Xing, H.** (2018). A large-sized basal ankylopollexian from East Asia, shedding light on early biogeographic history of Iguanodontia. *Science Bulletin*, *63*, 556–563. https://doi.org/10.1016/j.scib.2018.03.016

Associate Editor: Victoria Arbour